Coupling saturated and unsaturated flow: comparing the iterative and the non-iterative approach

Natascha Brandhorst[1], Daniel Erdal[2,3], and Insa Neuweiler[1]

[1]Institute of Fluid Mechanics and Environmental Physics in Civil Engineering, University of Hannover, Germany
[2]Center for Applied Geoscience, University of Tübingen, Germany
[3]Tyréns AB, Lilla Badhusgatan 2, 411 21 Göteborg, Sweden

Correspondence: Natascha Brandhorst (brandhorst@hydromech.uni-hannover.de)

Abstract. Fully integrated three dimensional (3D) physically based hydrologic models usually require many computational resources. For many applications, simplified models can be a cost effective alternative. 3D models of subsurface flow are often simplified by coupling a 2D groundwater model with multiple 1D models for the unsaturated zone. The crucial part of such models is the coupling between the two model compartments. In this work we compare two approaches for the coupling. One is iterative and the 1D unsaturated zone models go down to the impervious bottom of the aquifer and the other one is non-iterative and uses a moving lower boundary for the unsaturated zone. In this context we also propose a new way of treating the specific yield, which plays a crucial role in linking the unsaturated and the groundwater model. Both models are applied to three test cases with increasing complexity and analyzed in terms of accuracy and speed compared to fully integrated model runs. The non-iterative approach is faster ~~while the iterative approach is more accurate and robust. Besides,~~but does not yield a good accuracy for the ~~iterative coupling method a calibration of the specific yield is not needed.~~model parameters in all applied test cases whereas the iterative one gives good results in all cases. Which strategy is applied depends on the requirements: Computational speed vs. model accuracy.

1 Introduction

Three dimensional (3D) hydrologic models for subsurface flow are an important tool to gain a better understanding of the processes in a hydrologic system and to estimate the impact of possible future changes to it. However, these models tend to be very computationally demanding especially when applied to settings on large length scales that require a fine grid resolution (Kollet et al., 2010). Therefore, a lot of approaches to reduce the complexity of such models have been developed. One very common approach is to divide the model domain into two components: the saturated (groundwater) part and the

unsaturated part. This is often complemented by the assumption that flow in the unsaturated part occurs predominantly in vertical direction.

Thus, the unsaturated zone, which is usually the more complex one due to the strong nonlinearity of Richard's equation, can be represented by one or multiple one dimensional soil columns that can be solved independently from each other. Groundwater flow is then either modeled as 3D or as 2D depth integrated flow. The coupled model can then be seen as 2.5D or quasi 3D.

In this work we focus on phreatic aquifers where the crucial part is the coupling of the two model components. Usually, they are linked by the exchange of information on groundwater recharge and the position of the groundwater table. This can be done either in an iterative manner to account for the feedback between the two models (Shen Refsgaard and Storm, 1995; Shen and Phanikumar, 2010; Zhu et al., 2011; Kuznetsov et al., 2012; Xie et al., 2012; Xu et al., 2012; Mao et al., 2019; Zeng et al., 2019) or in a non-iterative manner without feedback (Pikul et al., 1974; Yakirevich et al., 1998; Beegum et al., 2018; Erdal et al., 2019). Both methods have been applied successfully. While iterative coupling in general yields a higher accuracy, non-iterative coupling requires less computational ressources (Zeng et al., 2019).

Differences among the coupling strategies exist also in terms of the spatial extent of the unsaturated zone model. Mostly, the unsaturated zone is modeled to span from the groundwater table to the land surface (Pikul et al., 1974; Yakirevich et al., Refsgaard and Storm, 1995; Yakirevich et al., 1998; Zhu et al., 2011; Kuznetsov et al., 2012; Xie et al., 2012; Zhu et al., 2012; Renard and Tognelli, 2016; Erdal et al., 2019; Zeng et al., 2019). As the groundwater table is moving with time, a remesh is needed after each coupling time step. Others assign a small overlap of the two model compartments which allows for a better calculation of the recharge flux (Xu et al., 2012; Beegum et al., 2018; Mao et al., 2019). A third approach is to consider 1D soil columns that reach down to the bottom of the groundwater domain (Shen and Phanikumar, 2010). Thus, the two compartments overlap in the entire saturated zone. The drawback of this approach is that the size of the unsatured model grid is increased. The advantage is that lateral fluxes in the groundwater can be passed directly to the unsaturated zone model and no remeshing is needed.

All these different coupling strategies have been tested successfully against real data or fully integrated 3D models. One has to keep in mind that there are limitations to the applicability that are not related to the coupling strategy but the general 2.5D or quasi 3D approach. Due to the 1D representation of the unsaturated zone, these models cannot be applied in the presence of large lateral fluxes in the unsaturated zone which might be the case in steep hillslopes. Furthermore, they neglect lateral water movement in the capillary fringe which can play a significant role.

One shared problem of these coupled models is due to the fact that the exchange quantities, e.g. recharge and water table position, are usually assumed to be constant over one coupling time step. This might lead to non-consistent model states when using a coupling scheme without feedback. While the consistency of the two model compartments is not necessary when the compartments are spatially separated, it is fundamental when they overlap. The easiest way to prevent these inconsistencies is to choose a small enough coupling time step, but this might lead to unfeasible compute times. Beegum et al. (2018) overcame this problem by updating the pressure head profile in the unsaturated zone after each time step in such a way that the new groundwater table position and the current recharge flux are both matched. By this procedure they prevent sudden in- or outflow of the unsaturated zone due to a stepwise changing groundwater table position. However, this requires the application of an optimization routine which can be rather time consuming. With an iterative coupling scheme, consistency can be achieved~~, but~~. In the MIKE-SHE model (Refsgaard and Storm, 1995), the water table is adjusted step-wise during the iterations until the mass balance is met with a predefined accuracy. But there still remains an error due to neglection of the temporal changes in the exchange information. Zeng et al. (2019) use linear extrapolation of the groundwater table position to reduce this error. Zhu et al. (2012) solve the two models jointly linked via the pressure head values at the interface. However, this is only possible if the groundwater model is 3D and the time steps in both compartments are equal. Often, the time step of the groundwater model is chosen to be larger than in the unsaturated model ~~where~~ smaller time steps are needed to achieve convergence for the nonlinear system of equations (Beegum et al., 2018).

Regarding the model consistency, another important factor is the quantification of the specific yield. It relates the ~~fluctuations of the groundwater table to the~~ amount of water being added or released to the fluctuations of the groundwater table, thus accounting for the neglected unsaturated zone. To get a consistent solution in both model parts in terms of water table position and mass conservation, it is obvious that a correct estimation of the specific yield in the groundwater model is needed.

~~However~~, the specific yield is not easy to be quantified as it depends on soil properties, change of the groundwater table and the water content profile above the groundwater table (Pikul et al., 1974; Sophocleous, 1985; Crosbie et al., 2005; Hilberts et al., 2005). The common approach to define it as drainage porosity and assign a temporally and often even spatially constant value is ~~clearly~~ a strong simplification in most applications. Beegum et al. (2018) performed a small sensitivity analysis on this parameter and detected a strong influence on the dynamics of the groundwater table position. Some research was dedicated to getting a better estimation of

this value in the context of groundwater modeling (Hilberts et al., 2005) and coupled saturated-unsaturated zone modeling (Pikul et al., 1974; Xu et al., 2012; Zeng et al., 2019). Hilberts et al. (2005) presented an analytical expression for the specific yield depending on the groundwater table position and the soil hydraulic parameters assuming hydrostatic equilibrium in the unsaturated zone. A similar approach was used by Crosbie et al. (2005) who propose a soil and depth dependent formulation of the specfic yield. Pikul et al. (1974) were the first to use a dynamic heterogeneous specific yield for linking the 1D unsaturated zone model with a 2D Boussinesq equation for the groundwater. They calculate it as the difference between saturated water content and the minimum water content at a specified depth. This approach was criticized by Vachaud and Vauclin (1975), who could confirm the dependency of the specific yield on space and time with physical experiments, but did not agree with its ambiguous definition proposed in the work by Pikul et al. (1974). Xu et al. (2012) implemented three different methods to define the specific yield when coupling the SWAP model (Kroes and Van Dam, 2003) with ~~MODFLOW-2000~~MODFLOW2000 (Harbaugh et al., 2000) but do not give a comparison of these methods or a suggestion. Zeng et al. (2019) distinguish between a small-scale and a large-scale specific yield. The small-scale specific yield is calculated from the unsaturated zone model as the change of water content up to a user specified elevation above the groundwater table, the large-scale specific yield is the commonly used parameter of the groundwater model. The difference between those two is used to correct the recharge flux. So the quantification of the specific yield remains an issue which is not yet fairly solved.

~~80~~ In this work we compare two different coupling methods for linking 1D unsaturated flow with 2D depth integrated groundwater flow. Both are quite simple, straight forward to implement and do not build on any additional software. One of them can keep the consistency of the two model compartments while still being fast and efficient whereas the other one is essentially designed to be very fast. The latter approach builds on the setup developed by Erdal et al. (2019) and uses a non-iterative, fast, but also rather approximate, coupling scheme, in which the unsaturated columns vary individually in length over the ~~sim-~~ ~~ulation~~simulation time. Hence, each column is resized every time step to fit the distance between groundwater table and surface. In the other method the unsaturated zone model covers the entire depth to the bottom of the groundwater domain and is coupled in an iterative manner to the groundwater model. Thus, the solution in both model compartments is guaranteed to be consistent. A new way of calculating the specific yield during the iteration is introduced and passed as coupling information between the model components. This prevents a prior calibration of this parameter and can account for its temporal and spatial variability.

We perform a sensitivity analysis to examine whether the calculated specific yield behaves reasonably and to identify those parameters which have a high impact on the groundwater dynamics in the coupled model. The number of parameters that need to be calibrated can thus be reduced saving computation time. As the equations describing unsaturated flow are nonlinear, a global sensitivity analysis, where the sensivity is measured over a larger (predefined) range of parameter values, is preferable. As global sensitivity metric we choose activity scores based on active subspaces introduced by Constantine and Diaz (2017). This is a rather new method that has been given increasing attention since its publication (Palar and Shimoyama, 2017; Fritz et al., 2019; Leon et al., 2019) and has also been used with subsurface models (Erdal and Cirpka, 2019). The idea of the method is to find the most influential directions in parameter space, in which the directions are linear combinations of the individual parameters, so called active variables.

The remainder of this paper is structured as follows: The coupled model with the two different coupling strategies as well as the activity scores used for the sensitivity analysis are described in detail in the following section. Afterwards the used test cases are introduced. We then present and discuss the results of the coupling scheme comparison and the sensitivity analysis. In the final part we give a summary of our experiments and conclusions.

2 Methods

2.1 Governing equations

The coupled model consists of two components, namely groundwater and unsaturated zone. Groundwater flow is modeled by the 2D Boussinesq equation for an unconfined aquifer

$$S_y \frac{\partial h}{\partial t} = \nabla \cdot (\overline{K_s}(h - z_0)\nabla h) + R \quad S_y \frac{\partial h}{\partial t} = \nabla \cdot (\overline{K_s}(h - z_0)\nabla h) + R \tag{1}$$

where S_y [−] is specific yield, h [m] is hydraulic head, t [s] is time, K_s [ms^{-1}] is the depth averaged saturated hydraulic conductivity, z_0 [m] is the bottom elevation of the aquifer and R [ms^{-1}] is groundwater recharge.

The mixed formulation of 1D Richards equation is used to describe flow in the unsaturated zone columns:

$$S(h_p)S_s \frac{\partial h_p}{\partial t} + \frac{\partial (S(h_p)\phi)}{\partial t} = \nabla \cdot (K(h_p)\nabla(h_p + z)) + Q \quad S(h_p)S_s \frac{\partial h_p}{\partial t} + \frac{\partial (S(h_p)\phi)}{\partial t} = \nabla \cdot (K(h_p)\nabla(h_p + z)) + Q \tag{2}$$

where S [−] is saturation, S_s [m^{-1}] is specific storage, h_p [m] is pressure head, φ [−] is porosity, K [ms^{-1}] is the unsaturated hydraulic conductivity, z [m] is the geodetic height above the bottom of the aquifer and Q [s^{-1}] is a source/sink term. The specific storage is here defined as $S_s = \frac{\phi}{V_t}\frac{\partial V_t}{\partial h_p}$ with V_t [m^3] being the total volume and assuming that $\frac{\partial \phi}{\partial h_p}$ is negligible. We use this formulation of Richards equation as it is consistent with Parflow (Kollet and Maxwell, 2006), which we use as fully integrated reference model, even though there might be more common formulations and the first term describing compressibility of the whole medium is not relevant for our examples.

The relation between pressure head, saturation and unsaturated hydraulic conductivity is represented by the van Genuchten-Mualem GenuchtenMualem model (Van Genuchten, 1980):

$$S(h_p) = \begin{cases} S_r + \frac{S_{sat} - S_r}{[1+(\alpha|h_p|)^n]^m} & \text{if } h_p < 0 \\ S_{sat} & \text{if } h_p \geq 0 \end{cases} \quad (3)$$

$$K(h_p) = \begin{cases} K_s S_e^{0.5}\left[1-\left(1-S_e^{1/m}\right)^m\right]^2 & \text{if } h_p < 0 \\ K_s & \text{if } h_p \geq 0 \end{cases} \quad (4)$$

where

$$S_e = \frac{S - S_r}{S_{sat} - S_r} \quad (5)$$

[−] is the effective saturation and the model parameter m [−] is usually given by $m = 1-1/n$. The model parameters α [m^{-1}] and n [−] are related to the pore-size distribution, S_{sat} and S_r [−] are the saturated and residual saturation, respectively.

2.2 Coupling

2.2.1 General approach

The coupled model The coupled model is a simplified subsurface model that can model flow in the groundwater and in the vadose zone, but no overland flow. It consists of a 2D depth averaged model for horizontal groundwater flow (Eq.1) and multiple 1D models for

~~125~~ vertical unsaturated flow (Eq.2). Each 1D model is located at a cell of the groundwater model grid. To reduce the computational burden not every groundwater grid cell has a 1D model. Instead, several grid cells of the groundwater model can be lumped

135 into zones that are assigned one 1D soil column. A schematic example of the model grid is shown in Fig.1. ~~The~~The atmospheric forcing of the unsaturated zone model as well as the recharge that is calculated from the unsaturated zone model and passed to the groundwater model ~~is~~are assumed to be constant within each zone. Therefore, the definition of the zones should be geared to land use, depth to groundwater table or other factors that affect

~~130~~ the recharge flux as also done by Xu et al. (2012), Renard and Tognelli (2016) and Erdal et al. (2019) and investigated by Zhu et al. (2012) and Zeng et al. (2019).

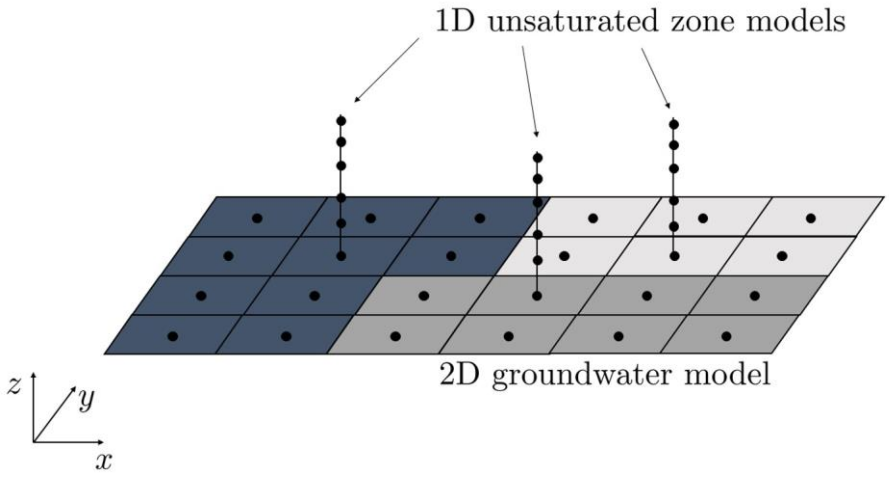

140 ~~Figure 1. Example of the coupled model grid with 3 recharge zones (white, gray and black).~~

Both components are discretized using finite volumes and an implicit Euler time integration. The nonlinear systems of equations are solved using the Newton Raphson scheme and line search. For the groundwater model a rectangular grid with uniform grid spacing is used. The 1D grid for the unsaturated zone can be non-uniform.

~~135~~ The boundary conditions on the lateral sides of the groundwater model can be either Neumann or Dirichlet boundary conditions. The upper boundary condition of the unsaturated zone models is a Neumann boundary representing the flux across the 145 land surface. In this work, the flux will be either precipitation or the net flux from precipitation and potential evapotranspiration

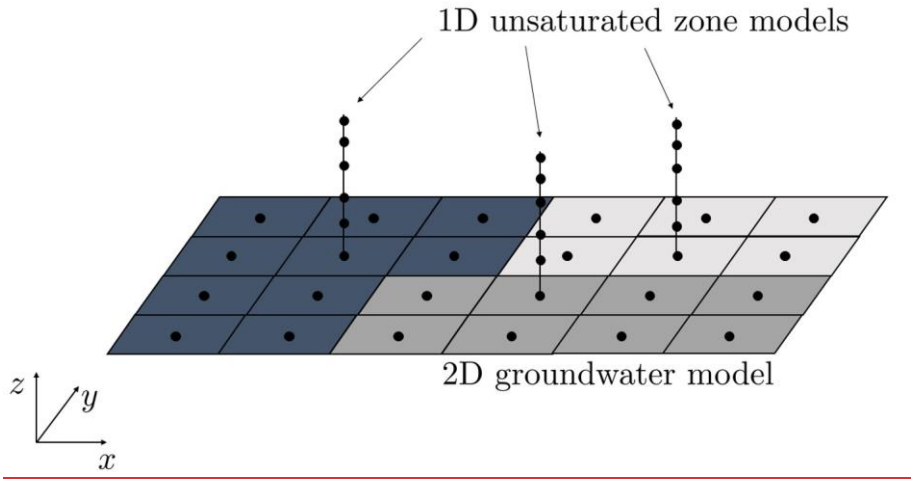

Figure 1. Example of the coupled model grid with 3 recharge zones (white, gray and black).

depending on the test case. The feedback from the groundwater model to the unsaturated zone models as well as the lower boundary condition of the unsaturated zone models depend on the coupling method described in the following sections.

The time step size of the unsaturated zone model is smaller than that of the groundwater model to guarantee convergence in the former but also numerical efficiency for the full model. The coupling time step, which defines the interval when the two model components exchange their information, is equal to the time step size of the groundwater model. All exchanged information such as groundwater recharge etc. is assumed to be constant during one coupling time step.

Both components as well as the coupling routine are implemented in Matlab.

2.2.2 Non-iterative method

The first coupling method aims at providing a fast and iterative free, but also rather approximate, solution to the numerical problem. A previous version of the model is published in Erdal et al. (2019). In this method, specific yield is a parameter of the groundwater model that the user needs to specify during model setup. Each unsaturated zone column is set up to range from the groundwater table to the land surface, with a Dirichlet boundary $h = 0\mathrm{m}$ at the bottom. A coupling time step is then performed as:

1. Run all unsaturated 1D column models for the coupling time step, collect the computed recharge (i.e. ~~flux~~fluxes leaving over

the bottom boundary for all 1D time steps during the coupling time step) and interpolate the 2D map of groundwater recharge.

2. Run the 2D groundwater model for the coupling time step with the computed recharge.
3. For each 1D column, resize all cells by a uniformed ratio computed such that ~~a~~the resized grid fits the new groundwater table to land surface distance at the column location. ~~All~~Thus, the cell sizes Δz are changed while all other properties of ~~the model are kept as they are, including saturation and hydraulic head.~~ the model are kept as they are, including saturation and hydraulic head which means a gain or loss of water in the 1D models.
4. Compute the amount of water lost (or gained) in each unsaturated model by resizing the grid.
5. Add (or subtract) a ratio r of this water to the recharge computed in the next coupling time step.
6. Move to the next coupling time step and repeat from point ~~i~~1.

The ratio r can in principle range from 0 to 1. At 1 the coupled model is locally mass conservative, as no water is lost or gained during the grid-resizing. However, a local mass-conservation in a non-iterative coupling method may not be wanted. Reasons for this are for example (1) the ~~groundwater table rise or fall~~water content in the unsaturated zone is also effected by lateral flows in the groundwater, (2) the added or subtracted water is only added in the next time step, (3) the dynamics around the rising or falling groundwater table is only captured in rough terms, and, (4) the column resizing is distributed across the full column. ~~In this work we compute r as the ratio between the incoming water from the 1D column ($R\Delta t_c$ [m]), the 1D column porosity (φ [−]) and the change of groundwater table elevation (ΔH_{GW} [m]):~~ This can cause numerical problems like oscillating groundwater tables. In this work we compute r as the ratio between the incoming water volume from the 1D column ($R\Delta t_c$ [m]) and the volume of water added to (or subtracted from) the groundwater ($\varphi \cdot \Delta H_{GW}$ [m]):

$$r_i = \min\left\{\left|\frac{R_i \Delta t_c / \phi_i}{\Delta H_{GW,i}}\right|, 1\right\} \quad \text{~~(5)~~}$$

$$r_i = \min\left\{\left|\frac{R_i \Delta t_c}{\phi_i \Delta H_{GW,i}}\right|, 1\right\} \quad (6)$$

where i is the index of the column, Δt_c [s] the coupling time step and r is limited to a maximum value of 1. The current formulation gives an indication to what extent the change of groundwater elevation can be attributed to the incoming groundwater ~~recharge. If recharge is the main contribution, the water lost in the resizing could be assumed to have entered the groundwater,~~

~~170~~180 recharge. If recharge is the main contribution, the water lost or gained in the resizing could be assumed to have entered/left the groundwater, while if the recharge is small but the change in groundwater table large, we find it more likely that the water may still be in the unsaturated zone ~~(e.g. the unsaturated zone is really compacted by a rise of groundwater levels).~~. We note that this is an ad-hoc solution, and that it differs to the one presented in Erdal et al. (2019), where r was simply set to 0. However, numerical tests show good stability and ~~better detailed~~the best overall performance for the applied test cases when r is computed as in this work even though a value of $r = 1$ would be needed to keep strict mass 185 conservation.

2.2.3 Iterative method

~~175~~ The second method couples the groundwater and the unsaturated model parts iteratively. Here, the 1D soil columns span the entire soil thickness from the impervious bottom of the aquifer up to the land surface. Thus, the 1D and the 2D model overlap in the saturated part. The bottom boundary condition of the 1D columns is then a no-flow boundary.

190 The groundwater recharge R [ms^{-1}], that is passed from the unsaturated zone models to the groundwater model, is defined - similar as in Crosbie et al. (2005) - as the amount of water being added to or substracted from the groundwater over time and ~~180~~ calculated from each unsaturated flow model as

$$R^{\nu} = \frac{\Delta H^{1}_{UZ} \cdot S^{\nu}_{y}}{\Delta t_c} R^{\nu} = \frac{\Delta H^{1}_{UZ} \cdot S^{\nu}_{y}}{\Delta t_c} \quad (7)$$

where H_{UZ} [m] is the position of the groundwater table in the unsaturated zone model, S_y [−] is the specific yield, Δt_c [s] 195 is the coupling time step and the superscript (ν) the iteration counter for the coupling time step loop.

~~is the coupling time step and the superscript (ν) the iteration counter.~~

The information passed from the groundwater model to the unsaturated zone models are the lateral fluxes Q_{lat} [ms^{-1}] into ~~185~~ or out of the columns cells. They are calculated at the locations where the unsaturated and groundwater models overlap as the amount of water being added to or substracted from the groundwater over time minus recharge:

$$Q^{\nu}_{lat} = \frac{\Delta H^{\nu-1}_{GW} \cdot S^{\nu-1}_{y}}{\Delta t_c} - R^{\nu-1} Q^{\nu}_{lat} = \frac{\Delta H^{\nu-1}_{GW} \cdot S^{\nu-1}_{y}}{\Delta t_c} - R^{\nu-1} \quad (8)$$

200 with H_{GW} [m] being the position of the groundwater table in the groundwater model. This cumulative flux is spread over the saturated part of the corresponding 1D model taking into account the variable cell sizes of the 1D grid:

190 $$q_{lat,i} = Q_{lat} \cdot \frac{\Delta z_i}{\sum_j \Delta z_j} q^{\nu}_{lat,i} = Q^{\nu}_{lat} \cdot \frac{\Delta z_i}{\sum_j \Delta z_j} \quad (9)$$

with $z_i, z_j \leq H_{UZ}$

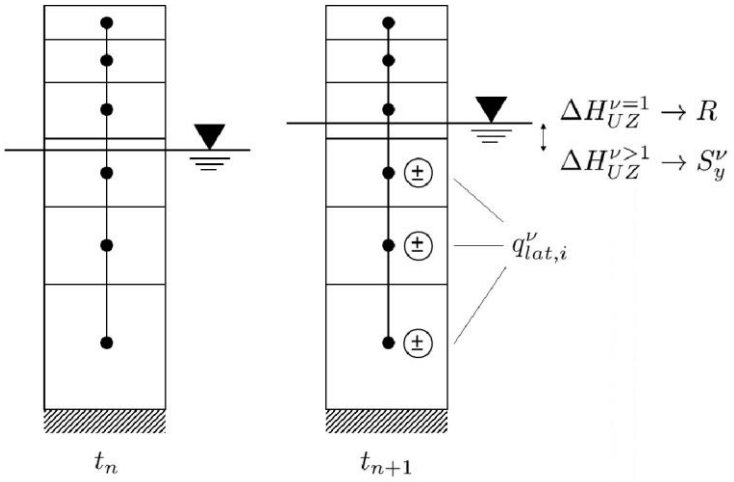

~~Figure 2. Illustrative example of the time step integration for one 1D model in the iteratively coupled model.~~

The local flux $q_{lat,i}$ [ms^{-1}] is given as a source/sink term to the i-th cell of the 1D model. This procedure is shown exemplarily for one 1D model in Fig.2.

205 In this approach, the position of the groundwater table in both models is not used as exchange information but as closure criterion for the iteration. With the lateral fluxes from groundwater flow being accounted for in the unsaturated zone models,

~~195~~ the calculated groundwater table position at the next time step should be equal in both models. However, this is only the case if the specific yield is chosen to correctly represent the ~~behaviour~~behavior of the unsaturated zone in the groundwater model. As was already discussed in the introduction, the specific yield is dynamic. Therefore it needs to be determined at every time step.

210 In the literature, different approaches of how to define and calculate the specific yield can be found. Most of them lack the dependency on the fluctuations of the groundwater table ΔH. The method proposed by Zeng et al. (2019) takes this into

~~200~~ account but requires the definition of a threshold elevation above the groundwater table. Here, we propose a method that ~~uses~~calculates the specific yield ~~as an adjustment parameter and calculate it~~ depending on ΔH without need of further user-defined parameters:

$$S_y^{\nu} = \frac{Q_{lat}^{\nu} \cdot \Delta t_c}{\Delta H_{UZ}^{\nu} - \Delta H_{UZ}^{1}} S_y^{\nu} = \frac{Q_{lat}^{\nu} \cdot \Delta t_c}{\Delta H_{UZ}^{\nu} - \Delta H_{UZ}^{1}} \quad (10)$$

215 It represents the ratio of the lateral fluxes and the corresponding change of the groundwater table position in the unsaturated zone model. In our case this is equivalent to relating all incoming fluxes ($Q_{lat}^{\nu} + R^{\nu}$) to the total change of the groundwater

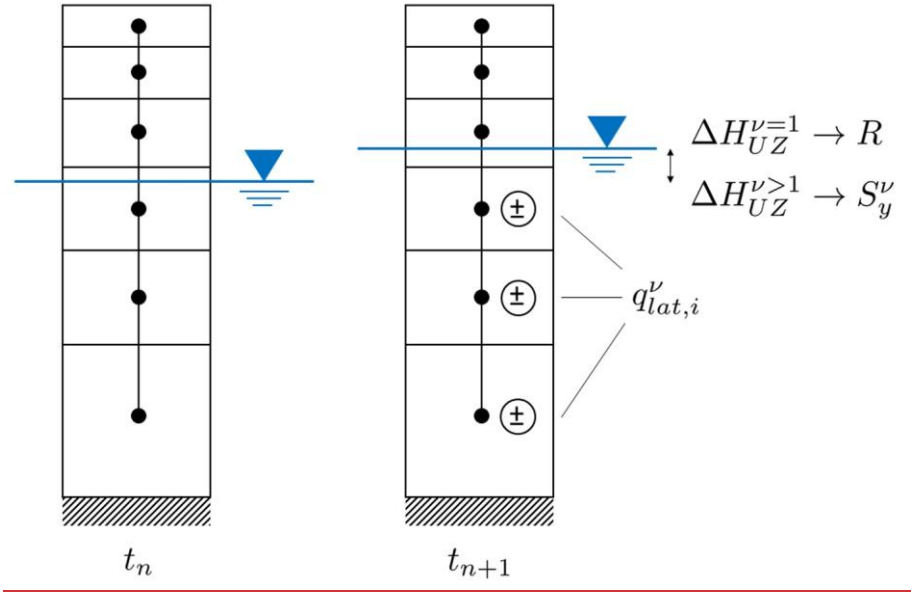

Figure 2. Illustrative example of the time step integration for one 1D model in the iteratively coupled model.

~~205 zone model. In our case this is equivalent to relating all incoming fluxes ($Q^{\nu}_{lat}+R^{\nu}$) to the total change of the groundwater~~ table position ($\Delta H_{UZ}{}^{\nu}$). ~~Using this value in~~So the ~~groundwater model~~specific yield is no longer a fixed model parameter but the ~~same lateral fluxes will cause the same response~~ratio of the ~~groundwater table in~~calculated water gain/loss per calculated groundwater level change where the water level change is calculated using the 1D Richards equation, which does not have the specific yield as a parameter. We thereby to a certain extent impose the unsaturated ~~and in~~zone model upon the

220 groundwater model. As the altered specific yield may lead to different lateral fluxes and consequently to a different specific yield, several iteration steps are needed to achieve a consistent solution in both model compartments. The convergence of the specific yield is - as in any numerical scheme - bound to an adequate choice of the numerical grid and in this case additionally to a sufficient number of unsaturated zone models. Note that if $\Delta^{H_{UZ}{}^{\nu}} - \Delta^{H_{UZ}{}^{1}} = 0\mathrm{m}$, then there are no lateral fluxes which means that there is no iteration ~~210~~required and the specific yield stays at its current value.

225 The integration of the coupled model to the next time step, which is illustrated in Fig.3, can be thus summarized as follows:

1. Run all unsaturated 1D column models for the coupling time step with $q_{lat,i} = 0\mathrm{ms}^{-1}\,\forall i$, calculate the computed recharge according to Eq.7 and interpolate the 2D map of groundwater recharge R^1.

2. Run the 2D groundwater model for the coupling time step with the computed recharge R^1.

3. ~~215 3.~~ Calculate the lateral flux source/sink terms ~~$q_{lat,i}^{\nu}$~~ $q_{lat,i}^{\nu}$ for the 1D models (Eq.9).

230 4. Run all unsaturated 1D column models for the coupling time step with ~~$q_{lat,i}^{\nu}$~~ $q_{lat,i}^{\nu}$, calculate the computed recharge according

~~4.~~ to Eq.7 and interpolate the 2D map of groundwater recharge R^{ν}.

5. Calculate and interpolate the 2D map of specific yield ~~S_y^{ν}~~ S_y^{ν} using Eq.10.
6. Run the 2D groundwater model for the coupling time step with the updated recharge R^{ν} and specific yield ~~S_y^{ν}~~ S_y^{ν}.
7. ~~220 7.~~ Repeat steps ~~(iii)~~3 to ~~(vi)~~6 until ~~$|H_{UZ}^{\nu} - H_{GW}^{\nu}| \leq \varepsilon_H$~~ $|H_{UZ}^{\nu} - H_{GW}^{\nu}| \leq \varepsilon_H$.

235 8. Move to the next coupling time step and repeat from point ~~i~~1.

~~Figure3 shows the iterative coupling procedure.~~ Note that an assumption is made in this approach. The source/sink terms $q_{lat,i}$ have an effect on the recharge ($R(Q_{lat} = 0)$ 6= $R(Q_{lat}$ 6= 0)), which due to the nonlinearity of Richards equation cannot be quantified. This effect is assumed to be negligible and the fluctuations due to recharge (ΔH_{UZ}^1) are kept constant during the iterations whereas the remainder of the total fluctuations ($\Delta^{H}_{UZ^{\nu}} - \Delta^{H}_{UZ^1}$) are assigned entirely to the lateral fluxes. Changes of the recharge R^{ν} during the iteration 240 are then only caused by changes of the specific yield (see Eq.7).

~~225 iterations whereas the remainder of the total fluctuations ($\Delta H_{UZ}^{\nu} - \Delta H_{UZ}^1$) are assigned entirely to the lateral fluxes.~~

Besides, as groundwater recharge and specific yield are calculated from the unsaturated zone models, they are ~~constant~~spatially uniform for all cells of the groundwater model that belong to the zone assigned to that unsaturated zone model. This leads to a simplified recharge and specific yield pattern but is necessary to keep the model computationally efficient.

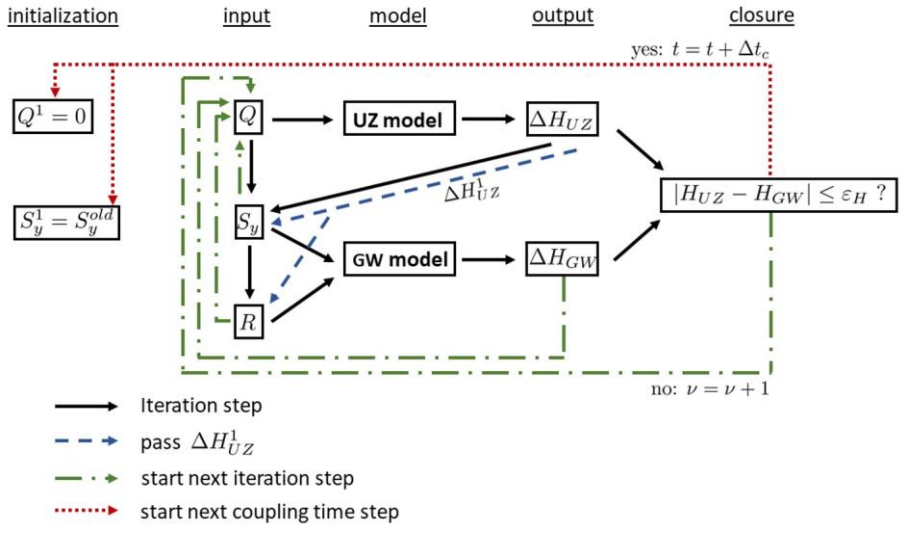

Figure 3. Flow diagram for the iterative coupling.

2.3 Activity scores

230245 We perform a global senstivity analysis to identify the most influential parameters for the groundwater dynamics in the two coupled models. As metric we use activity scores. Therefore (Constantine and Diaz, 2017). For this we define the vector of m model parameters x normalized to a range of $[0,1]$ with the probability density function $\rho(x)$ of the parameters and the scalar model output $f(x)$. The parameters and the model output f are defined in Sections 3.4 and 4.4, respectively. In our case, the parameters are the soil hydraulic parameters and the upper boundary condition, defined in more detail in Section 3.4. The model output f is either the groundwater table position, its daily fluctuation or the calculated specific 250 yield in the iterative model (see Section 4.4). The active subspace of f is defined by the eigenvectors of the matrix

The active subspace of f is defined by the eigenvectors of the matrix

Z

235 C = $\nabla f(x)\nabla f(x)^T\rho(x)dx = \mathrm{W}\Lambda\mathrm{W}^T$, (11)

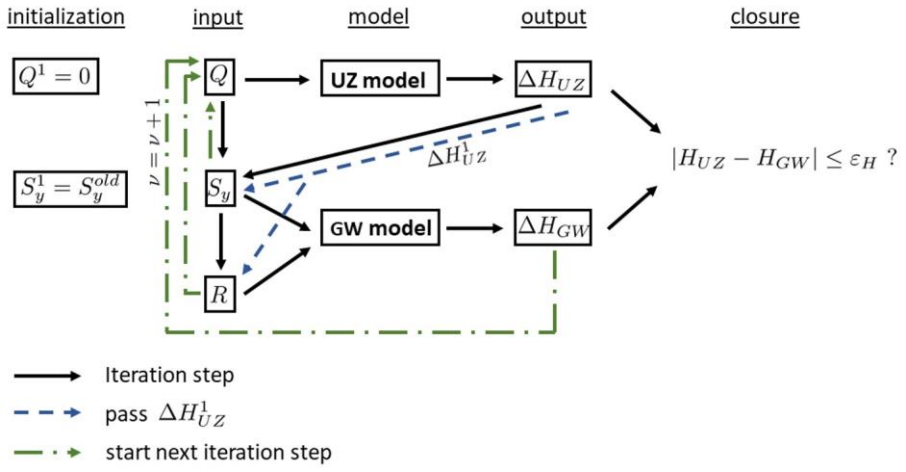

Figure 3. Flow diagram for the iterative coupling.

where W is the matrix of eigenvectors and Λ is the diagonal matrix of the corresponding eigenvalues λ_i in decreasing order. If there exists a λ_n that fulfills $\lambda_n \gg \lambda_{n+1}$, the individual sensitivity for the i th parameter can be calculated as $\lambda_n \gg \lambda_{n+1}$, Λ and W can be partitioned into

$$\Lambda = \begin{bmatrix} \Lambda_1 & \\ & \Lambda_2 \end{bmatrix} \quad a_i = a_i(n) = \sum_{j=1}^{n} \lambda_j w_{ij}^2$$

and $W = [W_1\ W_2]$, (12)

with Λ_1 containing the first n eigenvalues on its diagonal and W_1 consisting of the first n columns of W. The column span of W_1 is the active subspace of dimension n of the function f. The product $W_1^T x$ gives the n first active variables which are linear combinations of the normalized input parameters. A variation of an active variable causes a stronger variation in $f(x)$ than a variation of the inactive variables given by $W_2^T x$. Then, the individual sensitivity for the i-th parameter can be calculated as

$$a_i = a_i(n) = \sum_{j=1}^{n} \lambda_j w_{ij}^2 \quad (13)$$

where λ_j is the j-th eigenvalue and w_{ij} the value corresponding to the i-th parameter in the j-th eigenvector. This metric is called the activity score. For a transient problem, the activity score of a parameter can change with time, leading to a transient activity score $a_i(t)$.

In this work, the activity score is computed independently for each time step to create a transient score and normalized such that the sum of all scores at one time step is equal to one:

$$NAS_i(t) = \frac{a_i(t)}{\sum_{i=1}^{m} a_i(t)}. \quad (14)$$

Often, the integration over the parameter space required in Eq.11 is not feasible or not possible. Terefore, a Monte Carlo method

$$C \approx \frac{1}{M} \sum_{i=1}^{M} \nabla f(\boldsymbol{x}_i) \nabla f(\boldsymbol{x}_i)^T \quad (15),$$

where M samples are drawn independently from $\rho(x)$, is used to compute the matrix C as proposed in Constantine et al. (2015):

$$C \approx \frac{1}{M} \sum_{i=1}^{M} \nabla f(\boldsymbol{x}_i) \nabla f(\boldsymbol{x}_i)^T. \quad (15)$$

Another issue is related to the determination of ∇f. As this gradient often is unavailable, a common approach is to fit a polynomial model to relate the model output to the input parameters (Jefferson et al., 2015; Erdal and Cirpka, 2019). Following the suggestion by Erdal and Cirpka (2019), a second order polynomial depending on the input parameters is fitted to the data $f(x)$ using standard multiple regression, from which the gradient ∇f can be computed easily:

$$f(\boldsymbol{x}) \approx b_0 + \sum_{i=1}^{m} b_i x_i + \sum_{i=1}^{m}\sum_{j=1}^{m} b_{ij} x_i x_j \quad . \quad (15$$

$$f(\boldsymbol{x}) \approx b_0 + \sum_{i=1}^{m} b_i x_i + \sum_{i=1}^{m}\sum_{j=1}^{m} b_{ij} x_i x_j \quad . \quad (16)$$

3 Test cases

We test and compare the above described coupling methods using three different test cases. The first two test cases are taken from Beegum et al. (2018) where the second one was originally set up by Morway et al. (2013). As these are rather artificial, we added a third test case which is more complex and more realistic. The first test case is a flow model in a bucket setup where all boundary sides are closed. It represents a 1D flow problem consisting of two homogeneous soil layers with dynamic precipitation evapotranspiration (~~PET~~P-ET) data. It is used to investigate the coupling in the absence of any lateral fluxes where fluctuations of the groundwater table are only due to groundwater recharge. The second test case is conceptualized with a 3D model domain. However, as all parameters are constant over the length of the domain, it is effectively a 2D flow problem. Here again the soil is homogeneous, but it contains lateral fluxes. The third test case is similar to the second but the dimensions and the precipitation are modified such that the groundwater table falls during a certain period and the soil is made heterogeneous. This test case is a true 3D flow problem. The main features of the test cases are summarized in Table 1. For the 1D bucket model, one 1D soil column that is not coupled to groundwater is solved for comparison. The results of the other two test cases are compared to those obtained from a fully integrated 3D model set up with Parflow (Kollet and Maxwell, 2006).

Table 1. Main features of the three test cases.

	1D flow	2D flow	3D flow
soil heterogeneity	no	no	yes
lateral fluxes	no	yes	yes
rising and falling groundwater table	no	no	yes

simplified R and S_y pattern	no	no	yes

For the global sensitivity analysis a fourth test case is created which is mainly a combination of the second and the third test case. They are combined and modified in such a way that the groundwater table rises and falls, the simulation is long enough to finish the model spin up and parameters are homogeneous within each model compartment.

Grid convergence

We performed a convergence study on the spatial grid resolution ($\Delta x = \Delta y$ and Δz) and coupling time step size (Δt_c) for the three applied test cases using the iteratively coupled model. As we want to compare our results to those of Beegum et al. (2018),

Table 2. Soil hydraulic parameters for the three test cases for Parflow and the coupled model

	θ_r [–]	θ_s [–]	K_s [ms^{-1}]	α [m^{-1}]	n [–]	S_s [m^{-1}]	S_y[a] [–]
1D flow							
sand	0.045	0.43	$8.25 \cdot 10^{-5}$	14.5	2.68	0.0015	0.255
loam	0.004	0.43	$3 \cdot 10^{-6}$	3.6	1.6		
loamy sand	0.004	0.41	$7 \cdot 10^{-5}$	5.4	2.1		
loamy sand	0.057	0.41	$4.05 \cdot 10^{-5}$	12.4	2.28		
2D flow							
soil	0.1	0.45	$5.70 \cdot 10^{-4}$	1.65	2	0.0015	0.28
3D flow							
sandy clay	0.004	0.38	$3 \cdot 10^{-7}$	2.7	1.6	10^{-6}	0.28

a Only needed in the coupled model. Using the iterative coupling, this value is the initial value S_y^0.

we chose the grid sizes corresponding to the accuracy we obtained for the grid resolution used in their work (mean absolute error of the groundwater table over time of $MAE \leq 5 \cdot 10^{-3}\mathrm{m}$) for our final calculations. To guarantee the comparabilty among the fully integrated and the coupled model, we always use the same grid for the reference and for the coupled model using the two coupling schemes although one has to keep in mind that the vertical grid resolution in the non-iteratively coupled model

will change during the remeshing. The convergence study showed that in the vertical direction a much finer grid is needed with form factors up to 500. Besides, the third (heterogeneous) test case requires a finer horizontal grid to achieve the same accuracy as in the other two test cases. For all three test cases, the influence of the coupling time step Δt_c was negligible. Therefore, we decided to use the maximal possible value $\Delta t_c = 1\mathrm{d}$ (as we have daily changing forcing data in test case 1) for all test cases. The grid for the fourth test case used for the sensitivity analysis was not determined from a convergence study since its

accuracy does not need to be comparable to the other test cases and the convergence study might show different results for different parameter combinations. Instead, we chose a grid resolution between the second and the third test case, of which this test case is a mixture.

3.1 Test case 1: 1D flow

This model is taken from Beegum et al. (2018) and covers a domain of $1\mathrm{m} \times 1\mathrm{m} \times 10\mathrm{m}$. All lateral boundaries are ~~noflow boundaries. The net flux of daily varying precipitation and potential evapotranspiration shown in Fig.4 is applied as a~~ no-flow boundaries. The net flux of daily varying precipitation and potential evapotranspiration (P-ET) shown in Fig.4 is applied as a Neumann boundary at the soil surface. This data was collected at a weather station in Gdansk, Poland in 2011. The initial condition assumes a hydrostatic pressure profile in the lower $6.5\mathrm{m}$ of the soil corresponding to an initial position of the groundwater table at $3.95\mathrm{m}$ below the surface. In the upper $3.5\mathrm{m}$ of the soil, unit gradient flow is imposed by setting the pressure head ~~was set~~ to $-0.283\mathrm{m}$. The soil consists of two layers, a sandy soil in the top $2.5\mathrm{m}$ and a loamy sand soil underneath~~.~~ (see Fig.9). The soil hydraulic parameters for the two layers are given in Table 2. Since the groundwater table stays below the interface to the sandy soil layer during the entire simulation, the groundwater model is ~~assigned~~ assigned the loamy sand parameters.

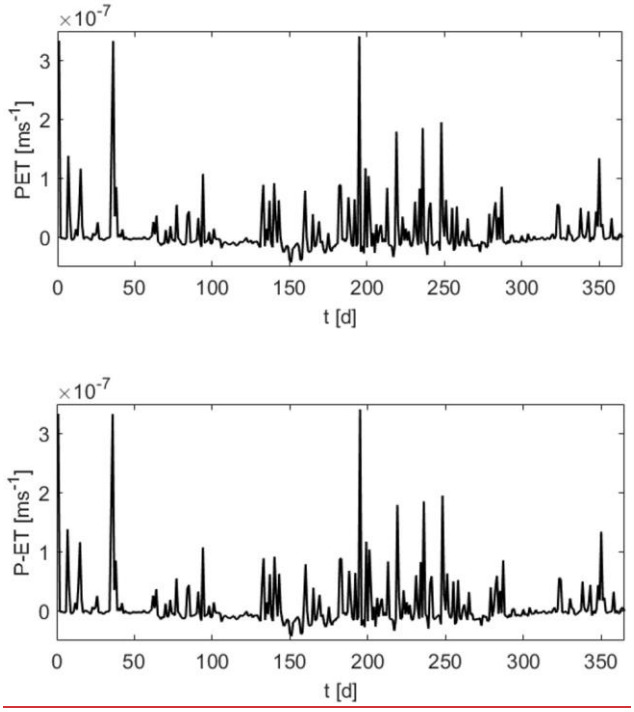

Figure 4. Net precitpitation and evapotranspiration used for the 1D flow model. Positive values indicate inflow, negative values outflow.

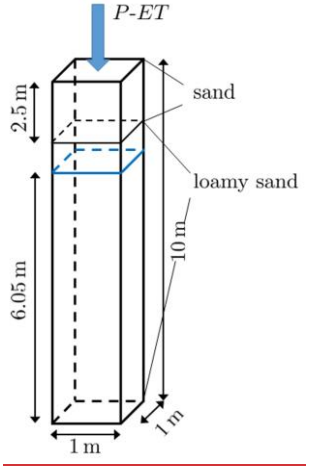

Figure 5. Model domain and initial water table position for the 1D flow model.

The total simulation time is one year. The 1D model used for comparison (pure Richards model, not coupled to groundwater) uses an adaptive time stepping scheme with a minimum value of 1s and a maximum value of 1h. The grid is

uniform with 1000 cells of 0.01m height. The same spatial resolution is used for the 1D models in the ~~iteratively coupled model. In the non-iterative model a grid consisting of 257 cells with variable grid size is used. As the 1D grids are remeshed after every time step in the non-iterative model, it is not necessary~~coupled model. The groundwater domain

~~280 to use the same spatial discretization as in the iterative model. The groundwater domain~~320 is divided into a 2×2 grid. Each groundwater cell is assigned a 1D model. The coupling time step as well as the time step of the groundwater model is set to 1d for both coupling methods. The time step for the 1D models is adaptive with a minimum value of 1s and a maximum value of 1d.

3.2 Test case 2: 2D flow

~~285~~ The dimensions of this model (Morway et al., 2013; Beegum et al., 2018) are 8000m × 4000m × 15m. Since there is no ~~variability~~vari-

325 ability along the 8000m side, flow is effectively 2D in this test case. There is a constant slope of 0.1% at the 4000m side. Two no-flow boundaries are assigned along the shorter side walls. On the other two sides there are Dirichlet boundaries corresponding to a groundwater table elevation of H = 7m and H = 0.9m at the top and the bottom of the slope, respectively (Fig.~~5~~6). The initial groundwater table elevation is interpolated linearly between the two Dirichlet boundaries. The initial ~~condi-~~condition for the

~~Table 2. Soil hydraulic parameters for the three test cases for Parflow and the coupled model~~

	θ_r [−]	θ_s [−]	K_s [ms^{-1}]	α [m^{-1}]	n [−]	S_s [m^{-1}]	S_y [−]
1D flow							
sand	0.045	0.43	$8.25 \cdot 10^{-5}$	14.5	2.68	0.0015	0.255
loamy sand	0.057	0.41	$4.05 \cdot 10^{-5}$	12.4	2.28		
2D flow							
soil	0.1	0.45	$5.70 \cdot 10^{-4}$	1.65	2	0.0015	0.28
3D flow							

unit 1	0.004	0.43	$3 \cdot 10^{-6}$	3.6	1.6	
unit 2	0.004	0.41	$7 \cdot 10^{-5}$	5.4	2.1	10^{-6} 0.28
unit 3	0.004	0.38	$3 \cdot 10^{-7}$	2.7	1.6	

a Only needed in the coupled model. Using the iterative coupling, this value is the initial value S_s^n.

290 tion for the 1D models is generated applying hydrostatic equilibrium and assigning a minimal initial pressure head of -1.25m. at locations

330 where the pressure head is below this value. Monthly varying rainfall (Fig. 67) is used as Neumann boundary condition for the land surface. The forcing is repeated for five cycles summing up to a total simulation time of five years. The soil parameters are listed in Table 2.

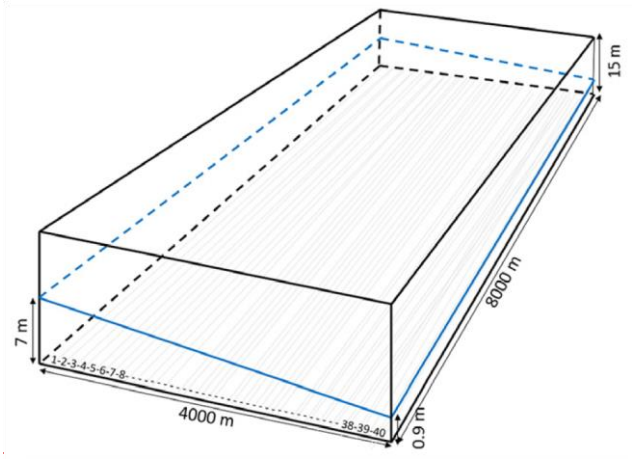

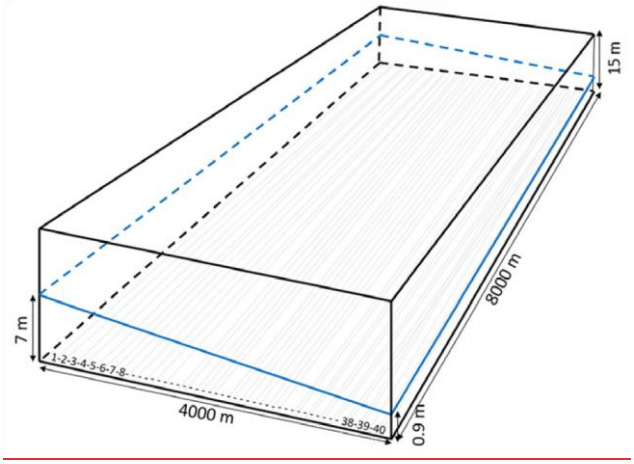

Figure ~~5~~6. Model domain and initial water table position for the 2D flow model. (Beegum et al., 2018)

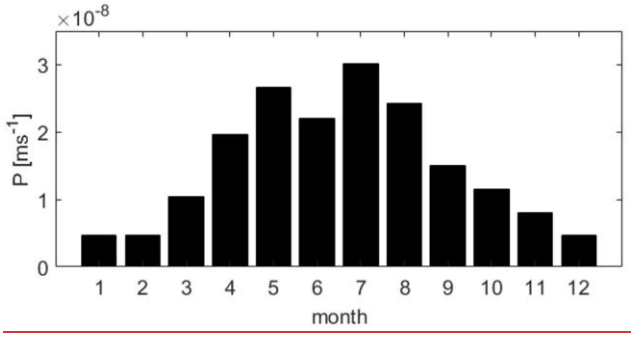

Figure 7. Net inflow used for the 2D flow model.

The 3D Parflow reference model uses a uniform grid with $80 \times 40 \times$ ~~150~~75 cells with grid size $\Delta x = \Delta y = 100\text{m}$ and $\Delta z =$ $0.$~~1m~~2m. The spatial resolution in the coupled model is the same with a 80×40 grid for the groundwater model and ~~150~~75 cells for ~~295~~ 335 the unsaturated zone models. The groundwater domain is divided into 40 zones all consisting of slices along the 8000m side

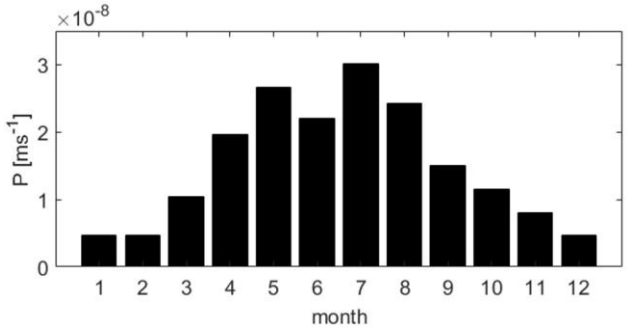

~~Figure 6. Net inflow used for the 2D flow model.~~

as shown in Fig.~~5~~6. With the flow problem being 2D this means that the entire domain is ~~acutally~~actually covered by 1D models. The coupling and groundwater time step is $\Delta t_c = 1\text{d}$ and the time step for the 1D models is again adaptive with a minimum value of 1s and a maximum value of 1d. Parflow uses an adaptive time scheme as well, with a maximum value of 1h.

3.3 Test case 3: 3D flow

~~300~~340 The first two test cases are rather simple. Therefore, a third test case is designed where the properties that are relevant for the coupling are closer to those of a model for a real hydrological system. The setup is similar to that of the second test case but with some modifications. The domain size is reduced to $800\text{m} \times 400\text{m} \times 15\text{m}$, the slope is maintained. The lateral

boundaries are the same, the flux boundary at the land surface now consists of three cycles of the precipitation shown in Fig.~~6~~7, followed by two no-flux years and then again two years using the original precipitation data. Thus, the total simulation time ~~is seven years. With~~

~~305~~345 is seven years. With these changes, the groundwater table is forced to eventually fall and then rise again. Apart from the more dynamic groundwater table, the influence of heterogeneities should be investigated with this test case. Therefore, instead of the homogeneous soil, three different soil ~~units~~types, representing loam, loamy sand and sandy clay, are distributed throughout the domain as depicted in Fig.~~7~~8. The distribution is synthetic and the corresponding parameter values are given in Table 2. In the coupled model, the parameters for the groundwater model are averaged arithmetically over the depth of the saturated zone in

350 that grid cell. This averaging takes place at every time step adapting to the new position of the groundwater ~~310~~ table. The initial condition is the same as in the 2D flow case.

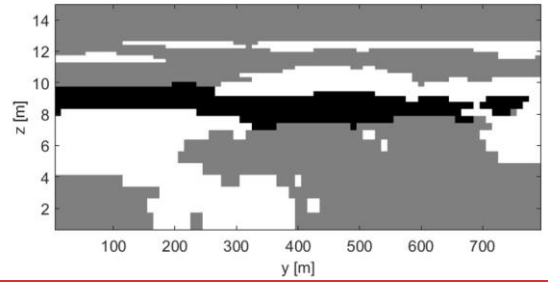

Figure 8. Distribution of soil types along the 800m side at x =195m in the 3D flow model. *grey:* loam, *white:* loamy sand, *black:* sandy clay.

The horizontal spatial resolution is increased to $\Delta x = \Delta y =$ ~~10m. In the~~5m. The vertical ~~direction a~~ grid consists of 200 cells and is non-uniform ~~grid is used~~ with ~~smaller~~ grid sizes ~~close to~~ranging between Δz_{min} = 0.75mm at the surface and ~~a total of 50 cells~~Δz_{max} = 0.3m at the bottom. The same resolution is used for Parflow and for the coupled model. With the heterogeneous soil, each grid cell of the groundwater model would need 355 a 1D model to cover the entire domain. As this is computationally not feasible, the groundwater domain is again divided into 40 zones but now spread evenly across the domain each covering an

~~315~~ area of ~~10×8~~20×16 grid cells. The 1D models are placed at the center of each zone and assigned the soil hydraulic parameters at this location. Thus, also the influence of a simplified recharge (and specific yield) pattern, which is constant within each zone and calculated from the corresponding 1D model, can be investigated. The time step sizes are the same as in the 2D flow model.

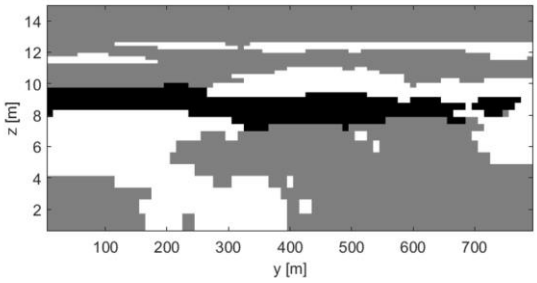

Figure 7. Distribution of soil units along the 800m side at x =195m in the 3D flow model. *grey:* unit 1, *white:* unit 2, *black:* unit 3.

3.4 Test case 4: sensitivity analysis

As already pointed out, for this test case the 2D and 3D flow test cases were combined. The domain size and the boundary conditions as well as the initial condition are the same as in the 3rd test case. This was done to maintain the rising and falling groundwater table. To get rid of spin up effects, the simulation time was increased, running four times the precipitation data used for the 3D flow case, adding up to a total simulation time of 28 years. The soil structure was simplified to be homogeneous within each model compartment, thus the groundwater model and the unsaturated zone models. For a heterogeneous soil structure a global senstivity analysis would be neither feasible nor very meaningful. The parameters included in the sensitivity analysis are listed in Table 3. Here, K_{GW} and K_{UZ} are the saturated hydraulic conductivity of the groundwater model and the unsaturated zone models, respectively, whereas the saturated part of the 1D models, that overlaps with the groundwater model, is also assigned the K_{GW} value. The parameters are sampled from uniform distribution functions ρ to cover their entire physically plausible range. Table 3 shows the limits of these ranges. Additionally, the influence of the upper boundary condition is investigated by multiplying the precipitation data with a constant factor r_{PET}. The residual saturation $S_r = \theta_r/\theta_s$ and the specific storage S_s are excluded from the analysis and set to 0.01 and 0.0015, respectively, as a previous smaller sensitivity analysis had shown no impact of these parameters (not shown). The range of the specific yield values is only valid for the non-iterative model. For the iterative model, the sensitivity towards the calculated specific yield is calculated, so the range is defined by the range of calculated values. Even though this is not a predefined parameter, its influence on the model output, i.e. the groundwater table dynamics, is of great interest and should be comprehensible and consistent over the entire simulation time.

Table 3. Parameter ranges for the parameters included in the sensitivity analysis. For the saturated hydraulic conductivity values for the groundwater (GW) and the unsaturated zone (UZ) model as well as the van Genuchten α the normal logarithm is sampled.

	K_{GW} [ms^{-1}]	S_y [−]	K_{UZ} [ms^{-1}]	α [m^{-1}]	n [−]	θ_s [−]	r_{PET} [−]
min.	$5 \cdot 10^{-7}$	0.05	$5 \cdot 10^{-7}$	0.5	1.5	0.05	0.75
max.	10^{-4}	0.7	10^{-4}	10	5	0.7	1.25

	K_{GW} [ms^{-1}]	S_y [−]	K_{UZ} [ms^{-1}]	α [m^{-1}]	n [−]	θ_s [−]	r_{PET} [−]
min.	$5 \cdot 10^{-7}$	0.05	$5 \cdot 10^{-7}$	0.5	1.5	0.05	0.75
max.	10^{-4}	0.7	10^{-4}	10	5	0.7	1.25

The horizontal spatial resolution is ~~again~~ $\Delta x = \Delta y = 10\mathrm{m}$~~, whereas~~ and the vertical resolution is $\Delta z = 0.1\mathrm{m}$ ~~as in the 2D flow case~~. As the sensitivity analysis requires a lot of model realisations, the number of unsaturated zone models and corresponding zones is decreased to eight to save computation time. Similar to the 2nd test case they are placed evenly along the $800\mathrm{m}$ side of the domain since the soil is homogeneous and flow thus 2D again. The time step sizes are the same as in the previously described test cases.

4 Results and Discussion

The coupling methods are compared in terms of accuracy and efficiency. The spatial and temporal distribution of the ~~ground-water~~groundwater table is used for the evaluation of the accuracy. The wall clock time serves as indicator for speed~~.~~ and is given in Table 4. No information about run times are given in Beegum et al. (2018). Therefore, their results are not included in the speed comparison. All Matlab calculations are done on a local desktop PC with an Intel Core i5 using 2 cores for the coupled model runs. The Parflow runs used for the other test cases are performed on the JUWELS supercomputer at the Research Centre Jülich which provides 2567 compute nodes with Dual Intel Xeon CPUs. 12 cores were used for the simulations.

Table 4. Wall clock times for the different test cases and coupling schemes.

	control run	iterative coupling (PC)	non-iterative coupling (PC)
1D flow	66s (Matlab, PC)	113s	39s
2D flow	11760s (Parflow, supercomputer)	630s	581s
3D flow	184680s (Parflow, supercomputer)	4857s	2262s

The iterative coupling uses a dynamic formulation of the specific yield. The resulting values are investigated in terms of plausibility. The groundwater table position, the groundwater table fluctuations and the specific yield calculated from the iterative coupling (all taken at the center of the domain) are used as observations $f(x)$ for the global sensitivity analysis. The resulting transient activity scores (Eq.~~13~~14) of the parameters listed in Table 3 are compared for the two coupling methods.

~~340~~ 4.1 Results 1D flow

~~Figure8~~Figure9 shows the water table elevation over time for the single column reference run and the two coupling schemes. The reference elevation $z = 0\mathrm{m}$ is located at $5\mathrm{m}$ below the surface. This is done to facilitate the comparison to the work by Beegum et al. (2018). Both, the iterative and the non-iterative coupling scheme show a good match with the single column run.

The accuracy of the iterative approach is slightly higher, no difference to the single column run can be seen in Fig.~~8~~9. A visual comparison indicates that the coupling applied by Beegum et al. (2018) yields a comparable accuracy.

The dynamic adaptation of the specific yield in the iterative coupling scheme is active only in the presence of lateral fluxes, because otherwise due to the formulation of the recharge in Eq.7 the groundwater table fluctutations in the two model compartments are already forced to be the same in the first iteration step. Therefore, in this test case the value stays constant at its initial value and further investigation is not possible.

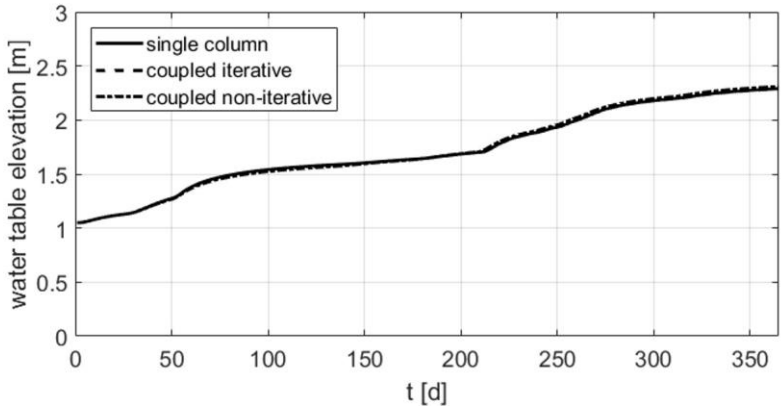

~~Figure 8. Groundwater table elevation over time for the 1D flow problem.~~

~~The wall clock times for the different methods are given in Table 4. No information about run times are given in Beegum et al. (2018). Therefore, their results are not included in the speed comparison. All Matlab calculations are done on a local~~

desktop PC with an Intel Core i7 using 4 cores for the coupled model runs. The Parflow runs used for the other test cases are performed on the JUWELS supercomputer at the Research Centre Jülich which provides 2567 compute nodes with Dual Intel Xeon CPUs. 12 cores were used for the simulations. For the 1D flow problem, the iterative coupling takes roughly twicethree times as 355 much wall clock time as the non-iterative coupling (see Table4). This is due to the larger grid of the iterative model which also includes the saturated part.

Table 4. Wall clock times for the different test cases and coupling schemes.

	control run	iterative coupling	non-iterative coupling
1D flow	40s (Matlab)	82s	35s
2D flow	12960s (Parflow)	799s	346s
3D flow	18000s (Parflow)	4215s	625s

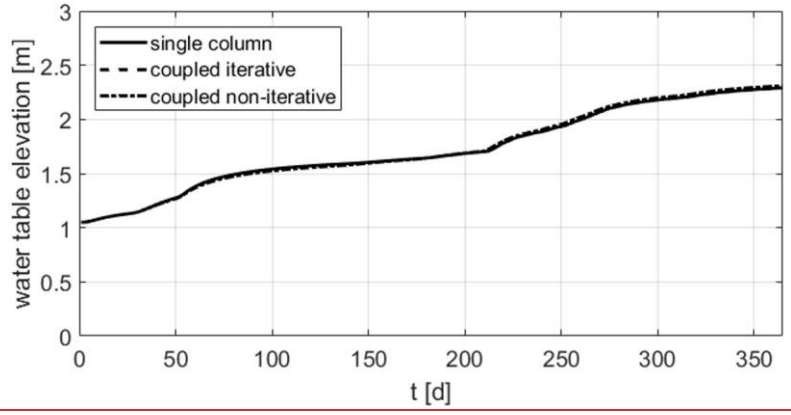

Figure 9. Groundwater table elevation over time for the 1D flow problem.

4.2 Results 2D flow

The temporal evolution of the groundwater table position at the center of the domain is shown in the upper plot of Fig.910. While both coupling approaches tend to overestimate the elevation of the groundwater table, increasing with time, the non-iterativenoniterative coupling shows a rather large offset compared to the Parflow run. This difference is also evident in the spatial plot of the groundwater table in the lower part of Fig.10. The overestimation of the iterative coupling scheme is also visible there, groundwater table in the lower part of Fig.9. The overestimation of the iterative coupling scheme is also visible there, but is clearly smaller. Besides, there is a shift in the shape of the groundwater table. The iterative coupling scheme shows the largest difference to the Parflow model close to the boundary at $x = 4000\mathrm{m}$ which will be discussed further in

~~Sec.4~~Section4.5. The largest difference between the non-iterative coupling and the Parflow run occurs at around $x = 1000\text{m}$. The results by Beegum et al. (2018) have a similar accuracy and shape as the results of the iterative coupling approach.

~~365~~ When considering the non-iterative model, it is notable that initial time steps are an issue, as the model starts almost ~~immediately~~imme-
415 diately with a too high groundwater table. However, the difference also grows slowly over time. Both of these issues occur as well when using smaller time step sizes and may be related to the reference model essentially acting as a bucket without any plausible steady state solution (i.e. steady state for the groundwater model would have groundwater tables far above the top of the domain). As such, an initial error in the model can never be compensated and will also lead to feedback effects, such as an overestimation of the groundwater recharge due to too short unsaturated zone model columns. In this respect, the 2D flow test
420 case is of limited use when evaluating simplified models for realistic setups.

~~370 too short unsaturated zone model columns. In this respect, the 2D flow test case is of limited use when evaluating simplified models for realistic setups.~~

The lateral fluxes in this setup cause a temporally and spatially changing value of the specific yield in the iterative model, which can be seen in the left plot of Fig.~~10~~11. However, the differences among the predefined zones (different lines) and also the temporal fluctuations are rather small. All values are smaller than the proposed value of 0.28, although the difference is less than 0.03. The temporal fluctuations of S_y suggest a dependence on the fluctuations of the groundwater table which also show

~~375 The~~ 425 a repeating pattern due to the cyclic forcing whereas its spatial differences ~~of the S_y values~~ indicate the dependence on the water table position ~~whereas its temporal fluctuations suggest a dependence on~~. The right plot of Fig.11 shows the ~~fluctuations of~~specific yield over the groundwater table ~~which also show a repeating pattern due to the cyclic forcing. Nevertheless, both effects are small here, which might be due to the homogeneity of the soil.~~

~~For this setup, again the non-iterative coupling is about two times faster than the iterative coupling (see Table 4).~~position. The ~~run time of the full 3D Parflow model is much higher.~~least squares regression line reveals

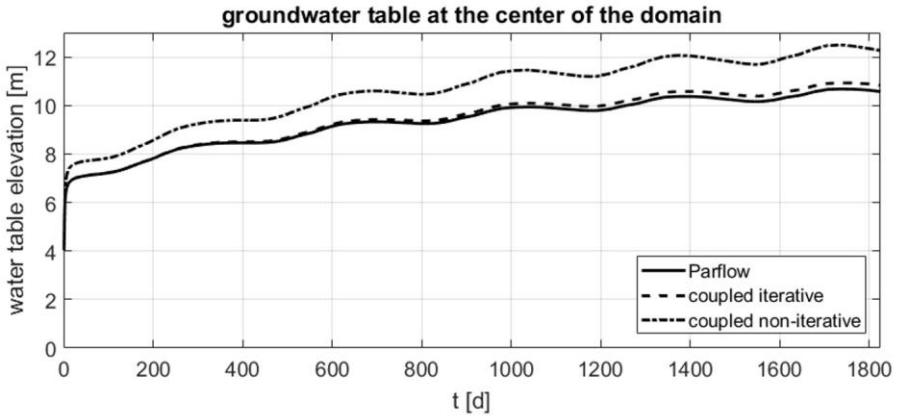
groundwater table at the center of the domain
water table elevation [m]
t [d]
Parflow
coupled iterative
coupled non-iterative

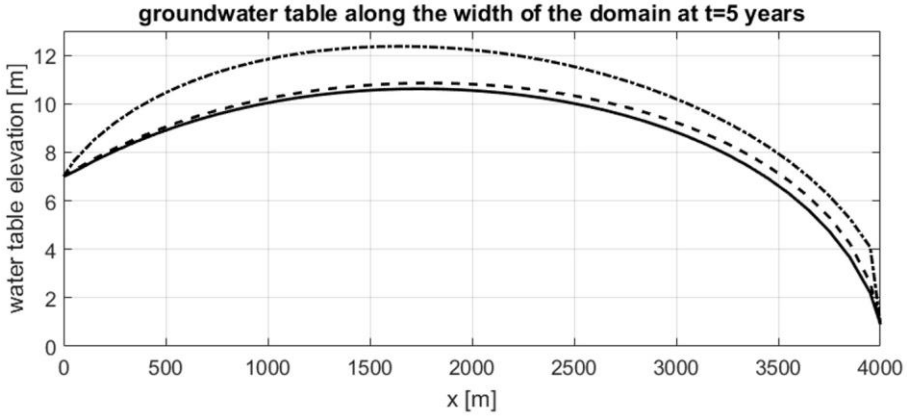
groundwater table along the width of the domain at t=5 years
water table elevation [m]
x [m]

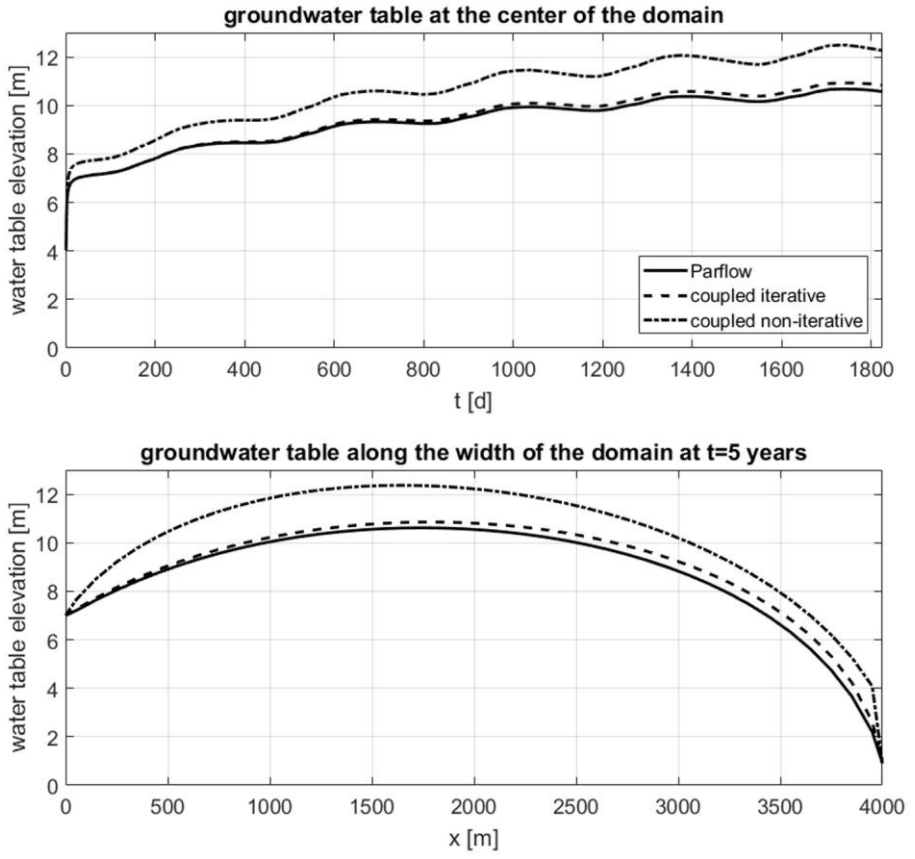

Figure ~~9~~10. Results of the 2D flow problem. *Upper:* Groundwater table elevation over time in the center of the domain. *Lower:* Groundwater table along the width of the domain at the final time step.

~~380 4.3 Results 3D flow~~

a linear relationship between these two variables, where S_y is increasing with increasing H_{GW}. Nevertheless, the temporal and the spatial differences of S_y are small here, which might be due to the homogeneity of the soil.

For this setup, again the non-iterative coupling is faster than the iterative coupling (see Table 4) but the difference is very 430 small, especially compared to the high run time used for the full 3D Parflow model.

4.3 Results 3D flow

In Fig.~~11~~12 the position of the groundwater table at the center of the domain is plotted over time (upper part). Both coupling schemes show a good agreement with the fully integrated 3D model. Similar ~~behaviour~~behavior is found at other positions in the domain.

The non-iterative scheme has a slight delay when the groundwater table is rising more rapidly, e.g. around $t = 1000\mathrm{d}$ and $t = 2250\mathrm{d}$. The groundwater table along the width of the domain ($y = 400\mathrm{m}$) at the end of the simulation is plotted in the lower part of Fig.12. Again, both coupling approaches match the Parflow result very well with small differences between

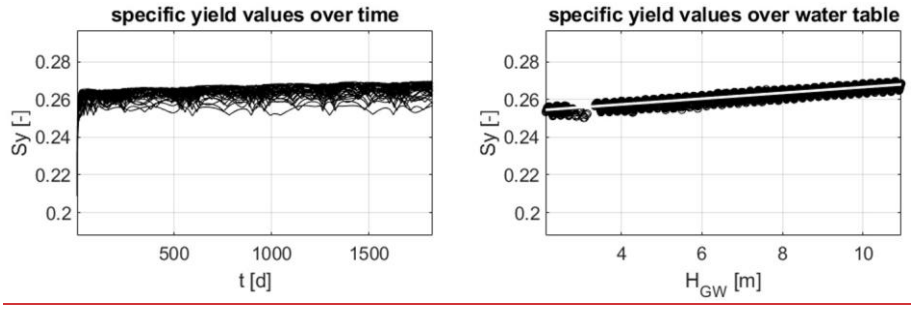

Figure 11. Specific yield values resulting from the iterative coupling for the 2D flow problem. *Left:* Specific yield over time. Each line corresponds to a 1D model and zone of equal recharge and specific yield in the groundwater model. *Right:* Specific yield over groundwater table position. The white line is the least squares regression line.

$x = 300\mathrm{m}$ and $x = 370\mathrm{m}$. The mismatch between the fully integrated and the coupled model is even smaller than in the less complex 2D flow case, which will be explained in the discussion part (Section 4.5).

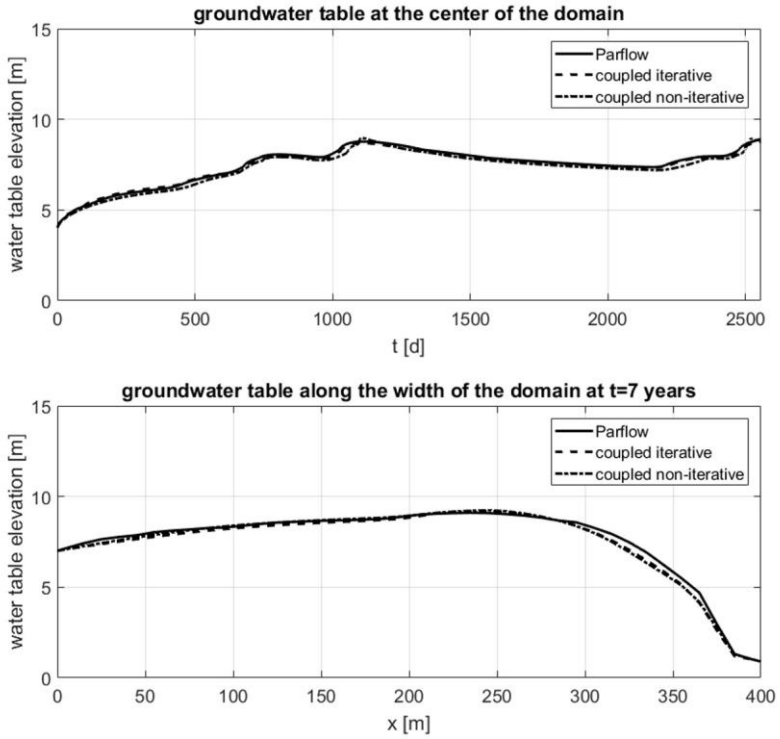

Figure 12. Results of the 3D flow problem. *Upper:* Groundwater table elevation over time in the center of the domain. *Lower:* Groundwater table along the width of the domain (y =400m) at the final time step.

~~385 the lower part of Fig.11. Again, both coupling approaches match the Parflow result very well with small differences between x = 300m and x = 370m.~~

The heterogeneity of the soil causes more variability of the groundwater table throughout the domain. ~~Figure12~~Figure13 shows the

440 difference between the groundwater table resulting from the coupled models and the full 3D model at the last time step in the entire domain. It can be seen that in the major part of the domain the differences are small~~. Areas with larger differences appear 390 at similar locations for both coupling schemes showing the largest deviations of up to ΔH_{GW} = 1.5m along the y = 800m~~ with an average deviation

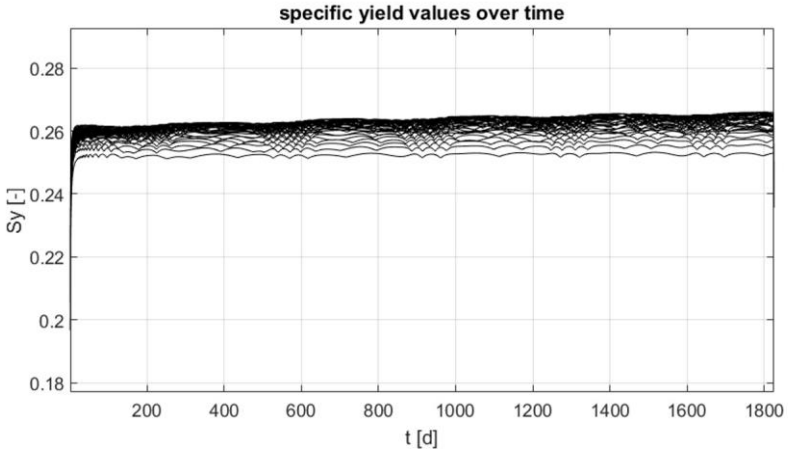

~~Figure 10.~~ _____ _____

of $\Delta H_{GW} = 0.12\text{m}$ for the iterative model and an average deviation of $\Delta H_{GW} = 0.16\text{m}$ for the non-iterative model. Areas with larger differences appear at similar locations for both coupling schemes showing the largest deviations close to the lower Dirichlet ~~Specific yield values resulting from the iterative coupling for the 2D flow problem. Each line corresponds to a 1D model and zone of equal recharge and specific yield in the groundwater model.~~

boundary~~.~~ (between $x = 300$ and $x = 400\text{m}$). Within these areas the differences between the iterative coupling and the Parflow model are smaller compared to the non-iterative coupling. The reason for these differences can be seen in Fig.14. The left plot shows the standard deviation of H_{GW} at the last time step within each zone corresponding to one 1D model obtained with the fully integrated model. The right plot shows the difference to this standard deviation obtained from the iteratively coupled model. It is evident that the variation of H_{GW} within one zone is much larger between $x = 300$ and $x = 400\text{m}$ than in the other parts of the domain. The lumping into zones of equal recharge, specific yield etc. reduces this variability in the coupled model, leading to larger differences compared to the fully integrated model in these areas. A higher accuracy could be achieved by using more 1D models but this would also increase the run times.

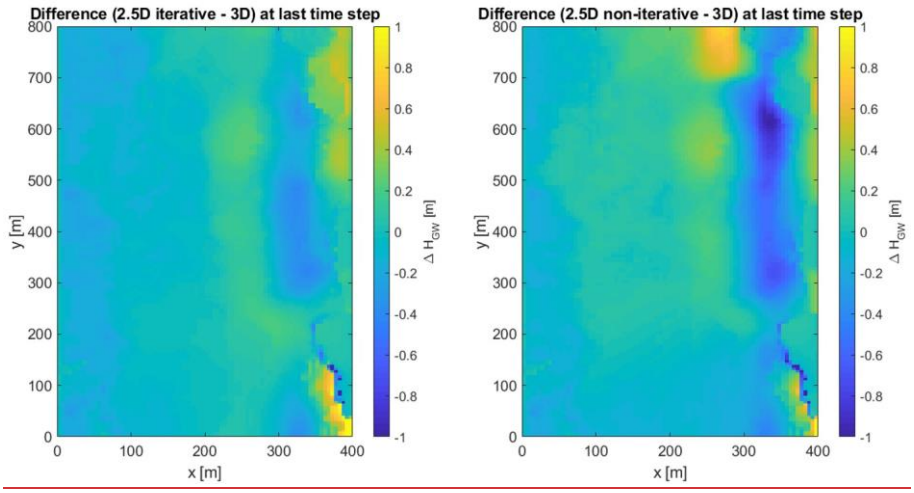

Figure 13. Difference of the groundwater table position compared to the full 3D run at the last time step. *Left:* Iterative coupling. *Right:* Non-iterative coupling.

The heterogeneity also leads to a larger variability of the specific yield in the iteratively coupled model as can be seen in the left plot of Fig.~~13~~15. There is a significant variation in space and time, with values ranging between approximately 0.01 and ~~0.7. Overall, the specific yield values are decreasing when~~ 0.33. A clear relationship between the groundwater table ~~is rising~~ and the specific yield with an increasing ~~when the groundwater table is falling (roughly between t = 1100d and t = 2200d).~~ ~~The ratio of the run times (Table 4) is different~~ S_y for ~~this~~ increasing H_{GW}, as in the 2D flow case, ~~with the iterative coupling using almost seven times more wall clock time than the non-iterative coupling. While~~cannot be seen here. Instead, the soil heterogeneities have a stronger impact on the S_y values. The right plot of Fig.15 shows the ~~Parflow model~~ normalized average specific yield and the ~~non-~~normalized average saturated hydraulic conductivity at the water table position $K_i = K_s(H_{GW})$. Both lines show a very similar temporal pattern and except for the time span between t = 1400 and t = 2500d their values are even close to each other.

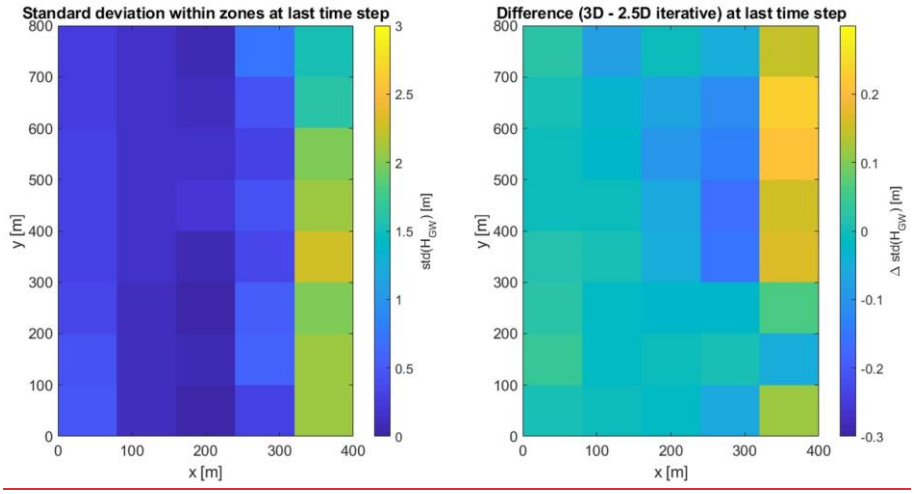

Figure 14. *Left:* Standard deviation of the groundwater table at the last time step within each zone corresponding to one 1D model in Parflow. *Right:* Difference of this standard deviation compared to the iteratively coupled model.

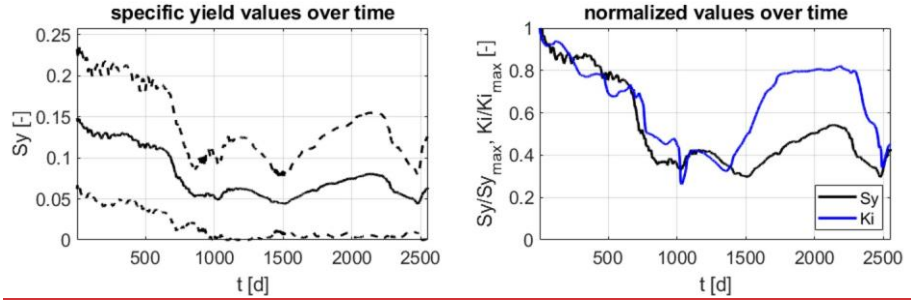

Figure 15. *Left:* Specific yield values resulting from the iterative coupling for the 3D flow problem. The solid line is the spatial average, the dashed lines indicate ± one standard deviation. ~~need less than twice the wall clock time than for the 2D test~~ *Right:* Normalized specific yield and saturated hydraulic conductivity at the water table position over time.

For this case~~, the wall clock time of~~ the iteratively coupled model ~~increases by a factor of five.~~

~~400 Still, both~~needs roughly twice as much run time as the non-iteratively coupled model (see 460 Table 4). Both coupled models are notably faster than the fully integrated 3D model.

4.4 Results GSA

A global sensitivity analysis is performed to identify the most influential parameters of the two coupled models regarding the groundwater dynamics, i.e. the groundwater table elevation H_{GW} and its daily fluctuation ΔH_{GW}, both taken at the center

of the domain. The resulting normalized transient activity scores NAS are plotted in the lower two plots of Figs.~~14~~16 and ~~15. The~~17.

~~405~~465 The upper plots of Figs.~~14~~16 and ~~15~~17 show the water table elevation and fluctuation of the iteratively coupled model averaged over all realisations, respectively. ~~All~~ Low values of the saturated hydraulic conductivity of the groundwater model K_{GW} result in a higher curvature of the groundwater table which in some cases reaches the land surface at the center of the domain. All these realisations ~~in which flooding occurs~~ are removed from the analysis as the model is not able to represent overland flow properly. Therefore, in the iteratively coupled model 316 out of initially 500 realisations are used and 395 in the non-iteratively coupled model.

~~Figure14~~470 Figure16 shows similar trends and patterns of the activity scores for the two coupling schemes. In both cases, the saturated ~~410~~ hydraulic conductivity of the groundwater domain K_{GW} is by far the most influential parameter, except for in the beginning.

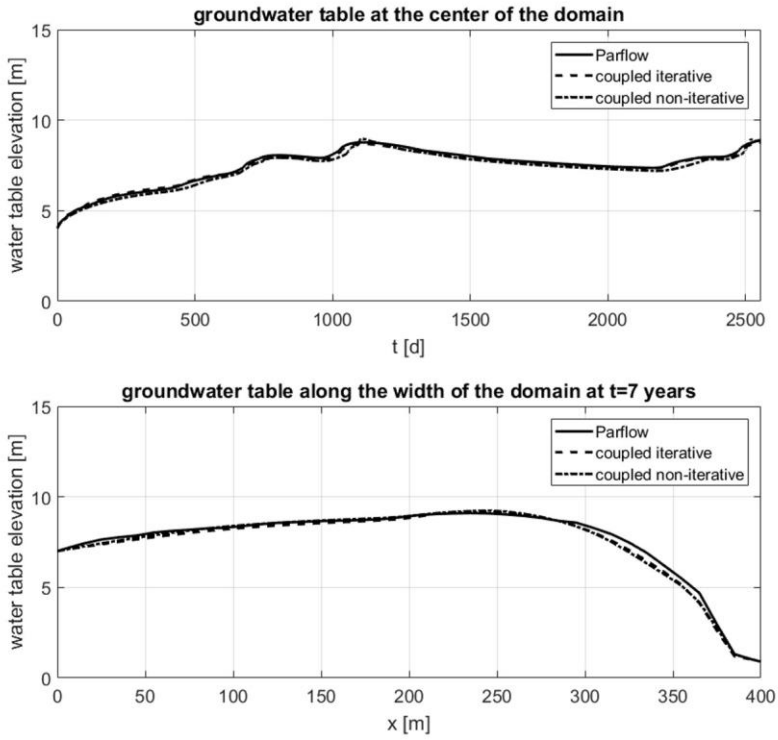

~~Figure 11 Results of the 3D flow problem. *Upper:* Groundwater table elevation over time in the center of the domain. *Lower:* Groundwater table along the width of the domain (y =400m) at the final time step.~~

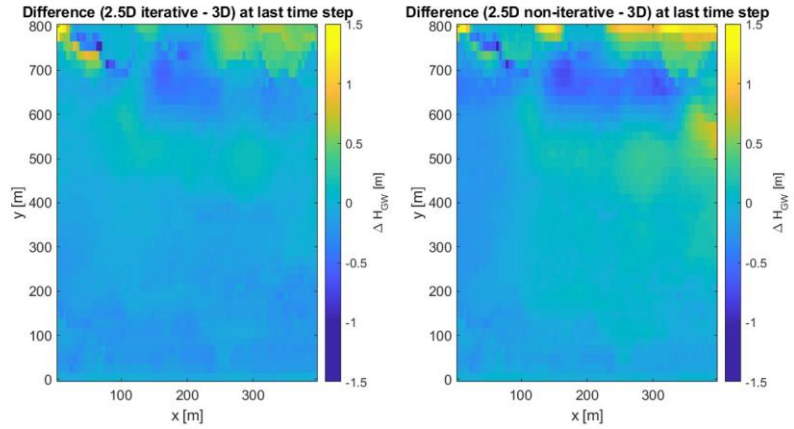

~~Figure 12. Difference of the groundwater table position compared to the full 3D run at the last time step. *Left:* iterative coupling. *Right:* non-iterative coupling.~~

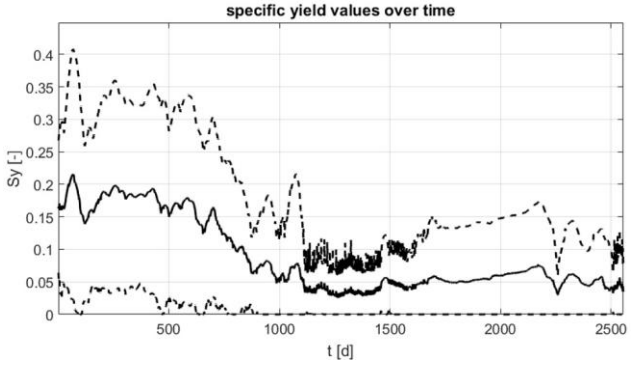

~~Figure 13. Specific yield values resulting from the iterative coupling for the 3D flow problem. The solid line is the spatial average, the dashed lines indicate ± one standard deviation.~~

There, the van Genuchten parameter α is dominant but its influence decreases with time. This is probably due to a spin up effect. When the model reaches the dynamic steady state (last two cycles), the influence of α has basically vanished. In the iteratively coupled model, porosity φ and the specific yield S_y still have a small influence, especially when the water table ~~starts to rise again after a draining period. Note that the specific yield in the iteratively coupled model is not the value used~~

~~415~~475 starts to rise again after a draining period. Note again that the specific yield in the iteratively coupled model is not the value used for the non-iteratively coupled model defined in Table 3 but the value calculated by the model during the simulation. In the non-iteratively coupled model there is also a slight sensitivity to the specific yield. All other parameters play a minor role.

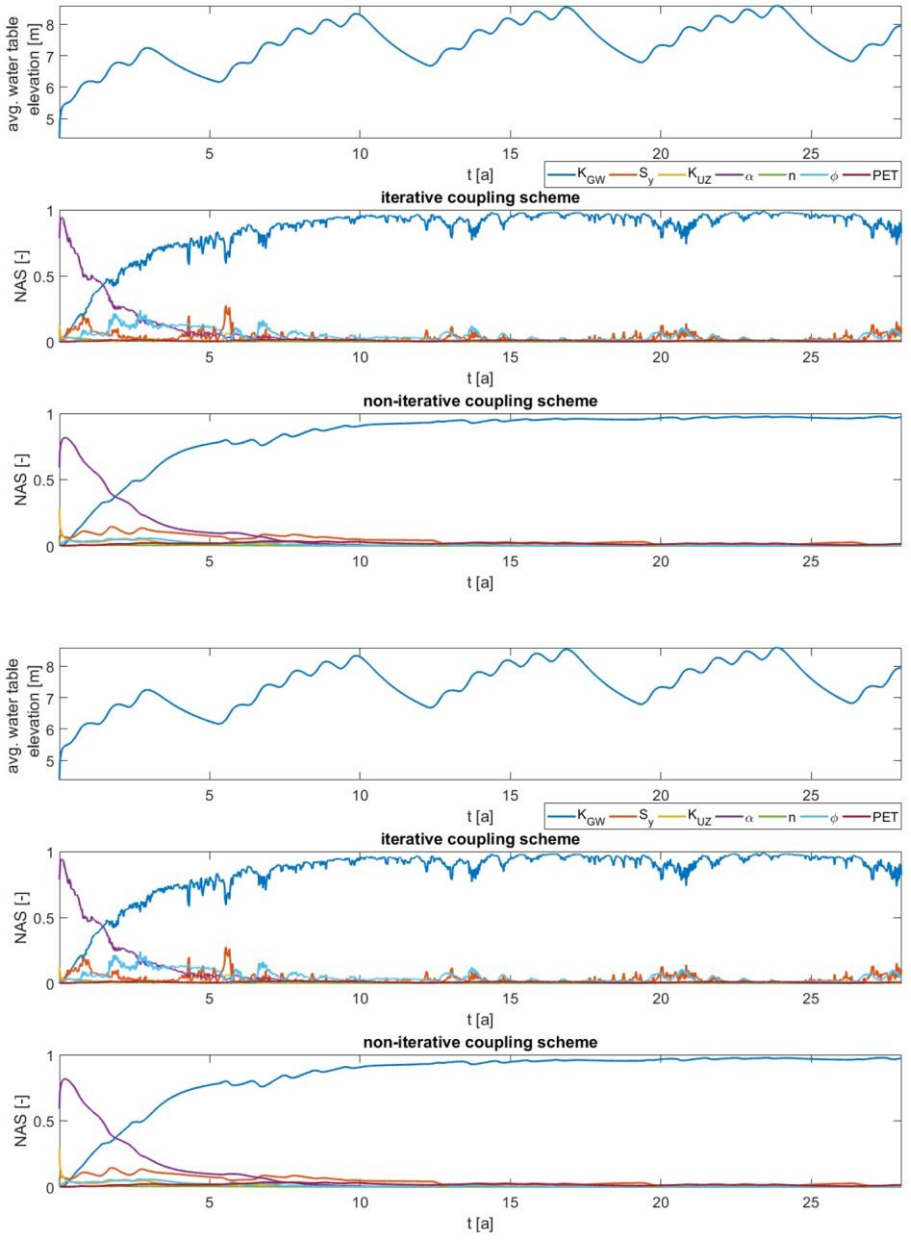

Figure ~~14~~16. *Upper plot:* Averaged water table elevation of the iteratively coupled model. *Lower plots:* Transient normalized activity scores for the two coupling methods.

The ~~acitivity~~activity scores concerning the water table fluctuations look different as can be seen in Fig.~~15~~17. Here, the most influential parameters are porosity φ, the saturated hydraulic conductivity of the groundwater model K_{GW} and the specific yield S_y.

The dominance of these parameters is alternating. The saturated hydraulic conductivity K_{GW} is the most important parameter during no rain periods. The fluctuations are then mainly caused by lateral fluxes, which depend strongly on this parameter. In the iteratively coupled model, when a high or low peak in ΔH_{GW} is reached, the recharge is the main driving force which is then mostly influenced by porosity. When looking at Eqs.1 and 7, one sees that S_y can be eliminated when lateral fluxes are negligible compared to the recharge fluxes, which explains why there is no influence of S_y under these conditions. These are the extreme conditions and inbetween the specific yield has the largest influence. At these times, there is also an increase in the influence of K_{UZ}. As will be shown later this is because the calculated specific yield mainly depends on this parameter. The results for the non-iterative model are very similar except for that the scores of porosity and specific yield follow a slightly different temporal pattern and the influence of the remaining parameters is a bit larger, but still rather small.

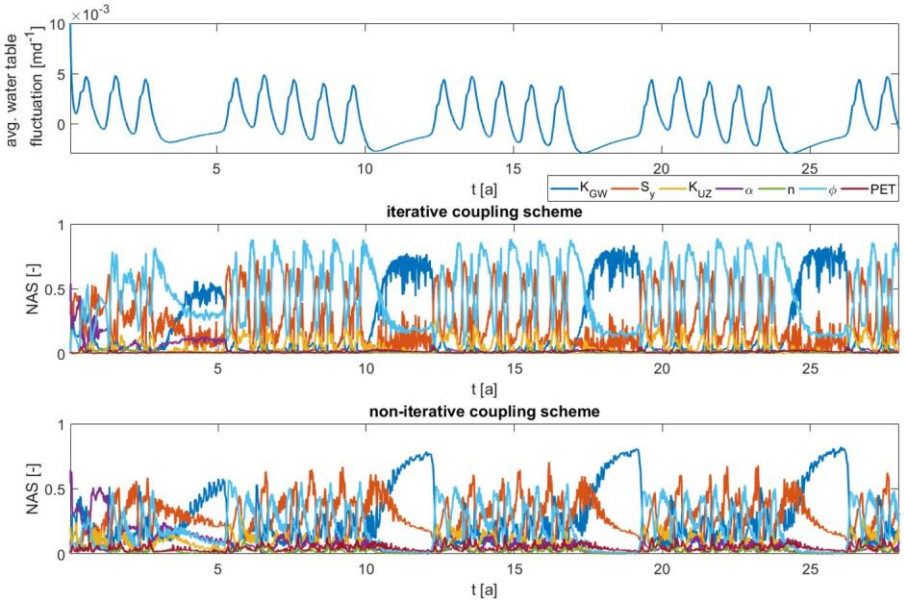

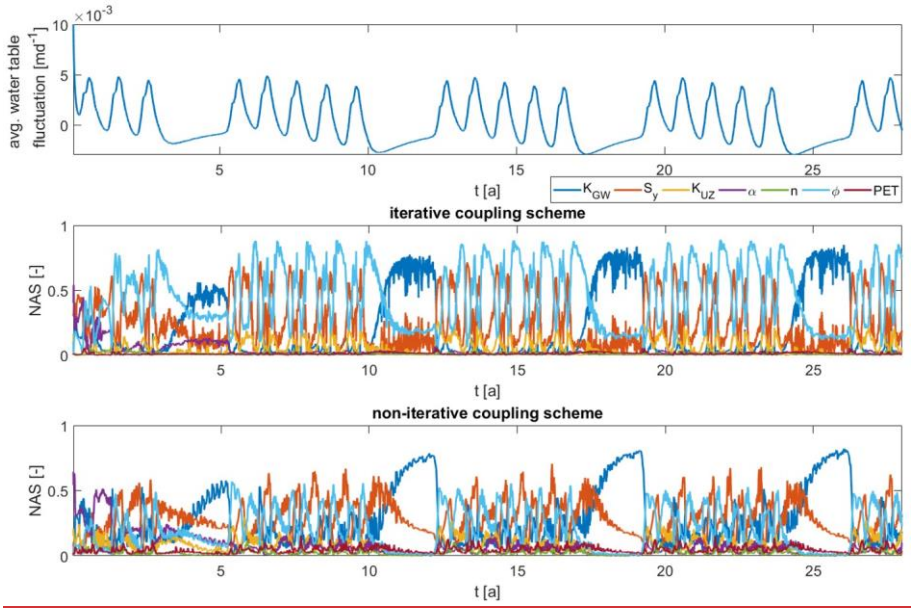

Figure ~~15~~17. *Upper plot:* Averaged water table fluctuation of the iteratively coupled model. *Lower plots:* Transient normalized activity scores for the two coupling methods.

~~Thus~~To analyze the sensitivity for different flow conditions, the observations (H_{GW} and ΔH_{GW} at the center of the domain) during the last seven year cycle, when the spin up is finished, are divided into three categories based on their average groundwater table position during that period: dry (3−7m), medium (7−11m) and wet (12−15m). For each category the normalized activity scores for the iteratively coupled model are calculated and averaged over time. These averaged scores are shown in Fig.18. The scores shown in Fig.16 and 17 correspond to the medium case. One can see that for both, the water table position and its daily fluctutation, the sensitivity towards the saturated hydraulic conductivity of the groundwater model is increasing with decreasing depth to groundwater table. Under drier conditions, the influence of porosity and the specific yield is stronger, especially regarding the water table fluctuation. Here, those two parameters become the most influential parameters while for the water table position, the dominance of K_{GW} remains. The influence of K_{UZ} on the water table fluctuations is also increasing with increasing depth to water table. Under drier conditions, the unsaturated zone parameters have a stronger impact on the recharge which explains this behavior. Interestingly, there is no increase of sensitivity towards the van Genuchten parameters α and n.

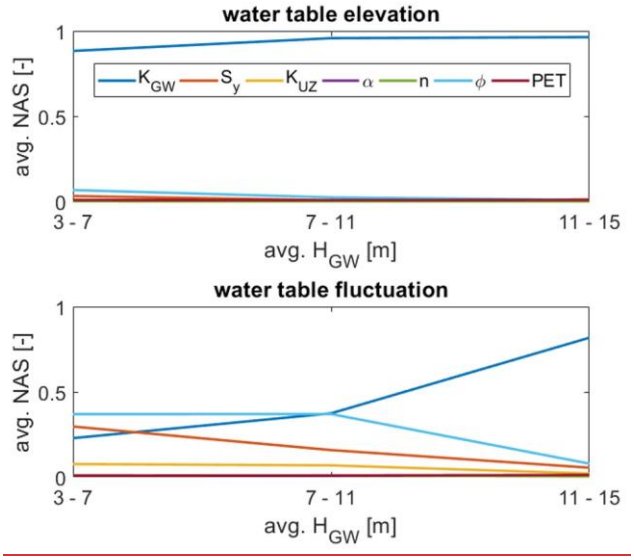

Figure 18. Averaged normalized activity scores of the last seven year cycle for the iteratively coupled model over the average water table position during that period. *Upper:* Normalized activity scores for the water table position H_{GW}. *Lower:* Normalized activity scores for the water table fluctuation ΔH_{GW}.

Overall, we see the importance of the specific yield for the groundwater table dynamics. With the iterative calculation of the specific yield a prior calibration of one of the most influential parameters is not needed. To see whether this calculated parameter behaves reasonably, a sensitivity analysis towards the calculated S_y at the center of the domain was conducted. The results are shown in Fig. 16.

19. Note that the S_y in the parameter list is now the initial value defined in Table 3 to which no sensitivity is expected. The average S_y value shows some smaller fluctuations, but overall it converges to a value around $S_y = 0.17$, which is a plausible value. The activity scores are also on the whole constant in time with the two most influential parameters being porosity φ and the saturated hydraulic conductivity of the unsaturated zone model K_{UZ}. The strong dependency on K_{UZ} is consistent with the results of the heterogeneous test case (see Fig.15). These two parameters are followed by the van Genuchten Genuchten parameters α and n, whose influence is already much smaller, though. Besides, there is a small influence of the saturated hydraulic conductivity of the groundwater model K_{GW}. This means that the specific yield is mainly depending on the unsaturated zone parameters. This is reasonable as its intention is to represent the missing unsaturated zone in the groundwater model.

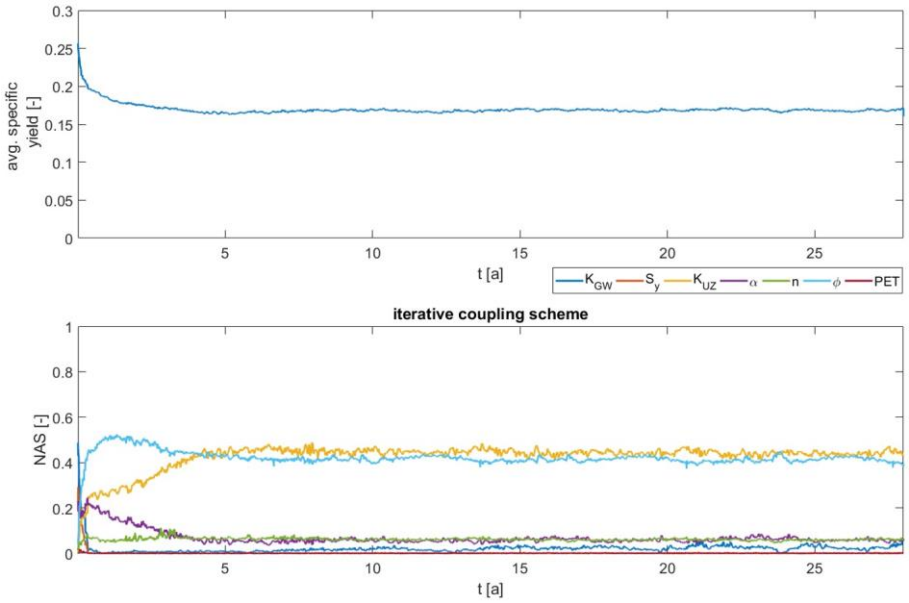

~~Figure 16. *Upper plot:* Averaged specific yield values of the iteratively coupled model. *Lower plot:* Transient normalized activity scores for the iterative coupling method.~~

4.5 Discussion

The above described numerical experiments show that both coupling methods presented in this work are well suitable to ~~440~~515 substitute a full 3D model under certain conditions. They can correctly capture the dynamics of the groundwater table in presence of lateral groundwater flow and soil heterogeneities. ~~Their accuracy is comparable to that of other coupling approaches (Beegum et al., 2018), but they are easy to implement, fast and in the case of the iterative model even consistent.~~The iterative model outperforms the fast but rather approximate non-iterative model in terms of accuracy for all applied test cases, especially in the second one. Its accuracy is comparable

~~In the second test case, the non-iterative method overestimates the groundwater table elevation notably, probably rooting in an overestimation~~

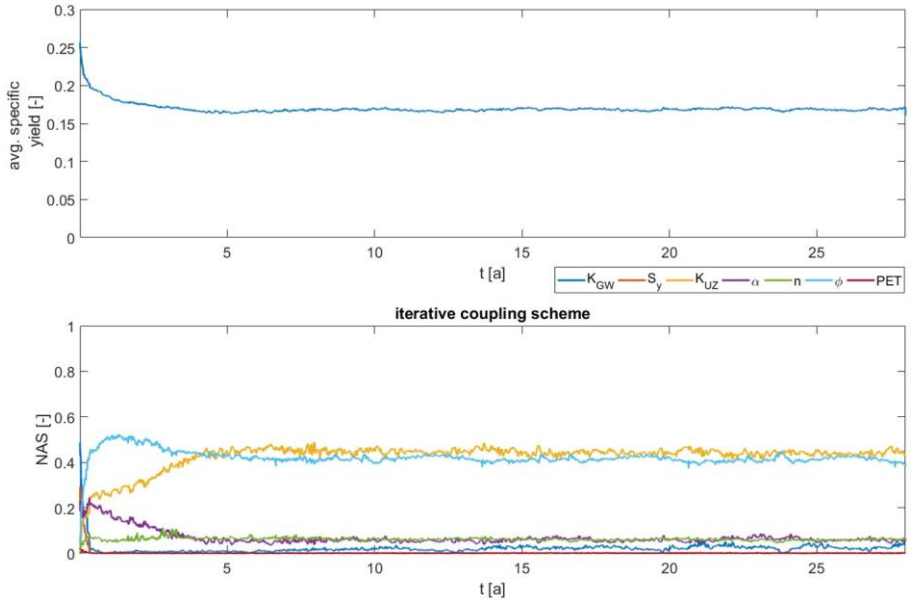

Figure 19. *Upper:* Averaged specific yield values of the ~~recharge flux. In the other test cases it also leads to slightly larger deviations from the 3D~~iteratively coupled model ~~than~~. *Lower:* Transient normalized activity scores for the iterative coupling ~~scheme. On the other hand, the higher accuracy of the iterative approach comes with a higher computational demand. Especially the heterogeneities in the third test case cause a large increase in run time compared to the non-iterative approach while the results are of comparable quality~~method.

~~A higher computational efficiency could be achieved by using less 1D models. On the contrary, using more models could help decreasing the discrepancies in the less accurate areas close to the no-flow boundary at $y = 800\text{m}$ which are most likely caused by the soil heterogeneities and the simplified recharge and specific yield pattern due to the zonation. As this is a general issue for these kind of models and does not relate to the presented coupling strategies themselves, we do not investigate it further. Another~~to that of other coupling approaches (Beegum et al., 2018), but it is easy to implement, fast and the model compartments are consistent.

One general problem of the coupled model can be seen in the second test case. Because of the low groundwater table and the large gradient at the lower Dirichlet boundary ($x = 400\text{m}$), water is also leaving the domain laterally via the unsaturated zone. This cannot be captured by the coupled model. The water thus has to first move vertically through the 1D

model before it can leave the domain through the groundwater. This leads to a pile-up of water and therefore an overestimation of the groundwater table along that boundary. This can also be seen in Beegum et al. (2018) which supports the assumption that it is a general issue.

In the 3D flow case (the third test case) the gradient at this boundary is smaller causing smaller lateral fluxes in the groundwater and thus also in the unsaturated part. Therefore the results of the coupled model are on average more accurate even though this test case is more complex than the 2D flow case. Here, on the other hand, we see the influence of the simplified recharge and specific yield pattern, which is however unavoidable for the efficiency of the coupled model.

The global senstivity analysis shows that the two coupled models behave reasonably and consistently among each other. The groundwater table position H_{GW} is mainly depending on the saturated hydraulic conductivity in the groundwater model K_{GW}. This was to be expected as it is the main parameter in the steady state formulation of Eq.1. The initially high and then decreasing influence of the van Genuchten parameter α indicates larger fluxes in the unsaturated zone at the beginning of the simulation. This is most likely due to the rather artificial initial condition in the unsaturated zone which ~~is constantly~~enforces unit gradient flow down to 1.25m above the groundwater table and no flow below. The temporal fluctuations of the groundwater table are

~~h_{UZ} = -1.25m at ≥ 1.25m above the groundwater table and needs to be corrected during the spin-up phase. The temporal fluctuations of the groundwater table are~~ influenced by more parameters, namely the saturated hydraulic conductivity in the groundwater model K_{GW}, the specific yield S_y and porosity φ. Which parameter is dominating depends on the current flow conditions as described in Section4.4.

The dynamic formulation of the specific yield in the iterative coupling approach allows the groundwater model and the unsaturated zone model to respond ~~comformably~~consistently to the given fluxes. So far this has been a challenge when using an overlapping coupling approach (Zeng et al., 2019). The specific yield values obtained in these experiments confirm the assumption that

it is depending on the saturation profile, the fluctuations of the groundwater table and the soil properties. However, these values should be interpreted with some caution. ~~This becomes evident when looking into~~In this model, the specific yield ~~values~~also needs to compensate the influence of the ~~3D flow problem.~~

~~Physically, a value larger than porosity is not possible. Here, the task of the specific yield is to represent the unsaturated zone in the groundwater model. A value that exceeds porosity means that a part of the water entering the cell laterally (if $Q > 0$) does not add to the groundwater but flows upward into the unsaturated zone. In case of a negative~~ lateral ~~flux, water would then be draining from the unsaturated zone. So actually this part is substracted from/added to~~fluxes on the recharge~~. If this effect can be accounted for correctly in the quantification of the recharge, the specific yield stays in its physically meaningful range. This is not the case in this model as we~~, which cannot ~~calculate this effect~~be quantified properly ~~and we therefore keep ΔH due to recharge fixed (see~~

~~480 Eq.7).~~

~~In the end, the specific yield is not a physical quantity but a model parameter. Therefore, it should be treated as such and fitted for each application. Calculating it within the iteration substitutes its calibration and is therefore an advantage over other methods~~. The sensitivity analysis for the parameters' influence on the calculated specific yield shows that it behaves reasonably ~~even~~, though ~~it can take unphysical values to compensate other effects.~~. It depends on the parameters of the unsaturated zone ~~485~~ models, especially on porosity φ and the saturated hydraulic conductivity K_{UZ}. The aim of the specific yield is to represent the missing unsaturated zone in the groundwater model, therefore a strong dependency on the unsaturated zone model's parameters is plausible. ~~So even though it is a model parameter, its values are meaningful.~~

5 Conclusions

In this work, two different ways of coupling a 2D groundwater model with multiple 1D unsaturated zone models are presented and compared in terms of accuracy and efficiency. The first approach uses a moving boundary formulation and couples the two domains non-iteratively. In the second approach they are coupled iteratively and the 1D models overlap with the groundwater model throughout the entire saturated part. A recalculation of the specific yield value during the iteration is applied to get to the same water table position in both model compartments.

The results and run times of the two coupling methods are compared to those of fully integrated model runs. ~~While the~~While the iterative coupling shows a higher accuracy, the non-iterative approach is faster. Both coupled models are significantly faster than the fully integrated model. Besides that, the iterative model ~~appears to be~~is more robust having a decent accuracy for all applied test cases, which is not the case for the non-iterative model, and can keep the consistency of the two model compartments.

A global sensitivity analysis revealed that the groundwater table position and its dynamics depend mainly on three parameters: the saturated hydraulic conductivity of the groundwater model, the specific yield and porosity. The specific yield is, however, hard to quantify especially because it is usually not constant over time, fluctuations can be large in the presence of soil heterogeneities. In the iteratively coupled model the specific yield is calculated by the model itself during the iterations accounting for this variability. It depends mainly on one additional parameter which is the saturated hydraulic conductivity

of the unsaturated zone model. This is an advantage of this method over other existing coupling strategies as this parameter is easier to be quantified and constant over time.

In general, both models qualify for substituting a fully integrated model when computational efficiency is more important than highly accurate results. The iterative approach is more robust and accurate and is recommended for most applications, while. When speed is essential, the usage of the non-iterative approach is better when speed is essentialmodel is also an option. Erdal et al. (2019) used a version of the here described non-iteratively coupled model successfully to reduce the compute time needed for model spin-up. Another application where such surrogate models can play an important role is data assimilation. Data assimilation often requires an ensemble of model realisations which comes with a strong computational burden. How well the here presented 2.5D model can replace a fully integrated model in this context is part of ongoing research.

Code and data availability. The MATLAB code to run the coupled model using the two presented coupling strategies and to visualize the output is available at http://doi.org/10.5281/zenodo.44225324737010. This code also includes the input and reference data for the three used test cases.

Author contributions. Simulations and code development were performed by DE and NB. IN acquired the funding. All authors contributed to the design of the experiments, the analysis of the results and writing the paper.

Competing interests. IN is a member of the editorial board of the journal.

Acknowledgements. This research is funded by the German Science Foundation (DFG) in the framework of research unit FOR 2131 under NE 824/12-1, and the Collaborative Research Center CAMPOS (CRC 1253 CAMPOS - Catchments as Reactors). Computing time has been provided by the Jülich Supercomputing Centre (http://www.fz-juelich.de)
provided by the Jülich Supercomputing Centre (http://www.fz-juelich.de)

References

Beegum, S., Šimu˚nek, J., Szymkiewicz, A., Sudheer, K., and Nambi, I. M.: Updating the Coupling Algorithm between HYDRUS and MODFLOW in the HYDRUS Package for MODFLOW, Vadose Zone Journal, 17, 2018.

Constantine, P. G. and Diaz, P.: Global sensitivity metrics from active subspaces, Reliability Engineering & System Safety, 162, 1–13, 2017.

Constantine, P. G., Emory, M., Larsson, J., and Iaccarino, G.: Exploiting active subspaces to quantify uncertainty in the numerical simulation of the HyShot II scramjet, Journal of Computational Physics, 302, 1–20, 2015.

Crosbie, R. S., Binning, P., and Kalma, J. D.: A time series approach to inferring groundwater recharge using the water table fluctuation method, Water Resources Research, 41, 2005.

Erdal, D. and Cirpka, O. A.: Global sensitivity analysis and adaptive stochastic sampling of a subsurface-flow model using active subspaces, Hydrology and Earth System Sciences, 23, 3787–3805, 2019.

Erdal, D., Baroni, G., Sánchez-León, E., and Cirpka, O. A.: The value of simplified models for spin up of complex models with an application to subsurface hydrology, Computers & Geosciences, 126, 62–72, 2019.

Fritz, M., Lima, E. A., Tinsley Oden, J., and Wohlmuth, B.: On the unsteady Darcy–Forchheimer–Brinkman equation in local and nonlocal tumor growth models, Mathematical Models and Methods in Applied Sciences, 29, 1691–1731, 2019.

Harbaugh, A. W., Banta, E. R., Hill, M. C., and McDonald, M. G.: MODFLOW-2000, The U. S. Geological Survey Modular Ground-Water Model-User Guide to Modularization Concepts and the Ground-Water Flow Process, Open-file Report. U. S. Geological Survey, 92, 134, 2000.

Hilberts, A. G., Troch, P. A., and Paniconi, C.: Storage-dependent drainable porosity for complex hillslopes, Water Resources Research, 41, 2005.

Jefferson, J. L., Gilbert, J. M., Constantine, P. G., and Maxwell, R. M.: Active subspaces for sensitivity analysis and dimension reduction of an integrated hydrologic model, Computers & Geosciences, 83, 127–138, 2015.

Kollet, S. J. and Maxwell, R. M.: Integrated surface–groundwater flow modeling: A free-surface overland flow boundary condition in a parallel groundwater flow model, Advances in Water Resources, 29, 945–958, 2006.

Kollet, S. J., Maxwell, R. M., Woodward, C. S., Smith, S., Vanderborght, J., Vereecken, H., and Simmer, C.: Proof of concept of regional scale hydrologic simulations at hydrologic resolution utilizing massively parallel computer resources, Water Resources Research, 46, 2010.

Kroes, J. and Van Dam, J.: Reference Manual SWAP; version 3.0. 3, Tech. rep., Alterra, 2003.

Kuznetsov, M., Yakirevich, A., Pachepsky, Y., Sorek, S., and Weisbrod, N.: Quasi 3D modeling of water flow in vadose zone and groundwater, Journal of Hydrology, 450, 140–149, 2012.

Leon, L. S., Miles, P. R., Smith, R. C., and Oates, W. S.: Active subspace analysis and uncertainty quantification for a polydomain ferroelectric phase-field model, Journal of Intelligent Material Systems and Structures, 30, 2027–2051, 2019.

Mao, W., Zhu, Y., Dai, H., Ye, M., Yang, J., and Wu, J.: A comprehensive quasi-3-D model for regional-scale unsaturated–saturated water flow, Hydrology and Earth System Sciences, 23, 3481–3502, 2019.

Morway, E. D., Niswonger, R. G., Langevin, C. D., Bailey, R. T., and Healy, R. W.: Modeling variably saturated subsurface solute transport with MODFLOW-UZF and MT3DMS, Groundwater, 51, 237–251, 2013.

Palar, P. S. and Shimoyama, K.: Exploiting active subspaces in global optimization: how complex is your problem?, in: Proceedings of the Genetic and Evolutionary Computation Conference Companion, pp. 1487–1494, 2017.

555 Pikul, M. F., Street, R. L., and Remson, I.: A numerical model based on coupled one-dimensional Richards and Boussinesq equations, Water Resources Research, 10, 295–302, 1974.

Refsgaard, J. and Storm, B.: Computer models of watershed hydrology, Water Resources Publications, pp. 809–846, 1995.

Renard, F. and Tognelli, A.: A new quasi-3D unsaturated–saturated hydrogeologic model of the Plateau de Saclay (France), Journal of 620 Hydrology, 535, 495–508, 2016.

Shen, C. and Phanikumar, M. S.: A process-based, distributed hydrologic model based on a large-scale method for surface–subsurface 560 coupling, Advances in Water Resources, 33, 1524–1541, 2010.

Sophocleous, M.: The role of specific yield in ground-water recharge estimations: A numerical study, Groundwater, 23, 52–58, 1985.

Vachaud, G. and Vauclin, M.: Comments on "A numerical model based on coupled one-dimensional Richards and Boussinesq equations" by 625 Mary F. Pikul, Robert L. Street, and Irwin Remson, Water Resources Research, 11, 506–509, 1975.

Van Genuchten, M. T.: A closed-form equation for predicting the hydraulic conductivity of unsaturated soils, Soil Science Society of America 565 Journal, 44, 892–898, 1980.

Xie, Z., Di, Z., Luo, Z., and Ma, Q.: A quasi-three-dimensional variably saturated groundwater flow model for climate modeling, Journal of Hydrometeorology, 13, 27–46, 2012.

630 Xu, X., Huang, G., Zhan, H., Qu, Z., and Huang, Q.: Integration of SWAP and MODFLOW-2000 for modeling groundwater dynamics in ~~shallow water table areas, Journal of Hydrology, 412, 170–181, 2012.~~

shallow water table areas, Journal of Hydrology, 412, 170–181, 2012.~~570~~

Yakirevich, A., Borisov, V., and Sorek, S.: A quasi three-dimensional model for flow and transport in unsaturated and saturated zones: 1. Implementation of the quasi two-dimensional case, Advances in Water Resources, 21, 679–689, 1998.

Zeng, J., Yang, J., Zha, Y., and Shi, L.: Capturing soil-water and groundwater interactions with an iterativefeedback coupling scheme: New 635 HYDRYS package for MODFLOW, Hydrology and Earth System Sciences, 23, 637–655, 2019.

Zhu, Y., Zha, Y.-y., Tong, J.-x., and Yang, J.-z.: Method of coupling 1-D unsaturated flow with 3-D saturated flow on large scale, Water ~~575~~ Science and Engineering, 4, 357–373, 2011.

Zhu, Y., Shi, L., Lin, L., Yang, J., and Ye, M.: A fully coupled numerical modeling for regional unsaturated–saturated water flow, Journal of Hydrology, 475, 188–203, 2012.